

# Generative Multiple-purpose Sampler for Weighted M-estimation

Minsuk Shin, Shijie Wang and Jun S Liu

## Abstract

To overcome the computational bottleneck of various data perturbation procedures such as the bootstrap and cross validations, we propose the *Generative Multiple-purpose Sampler* (GMS), which constructs a generator function to produce solutions of weighted M-estimators from a set of given weights and tuning parameters. The GMS is implemented by a single optimization without having to repeatedly evaluate the minimizers of weighted losses, and is thus capable of significantly reducing the computational time. We demonstrate that the GMS framework enables the implementation of various statistical procedures that would be unfeasible in a conventional framework, such as the iterated bootstrap, bootstrapped cross-validation for penalized likelihood, bootstrapped empirical Bayes with nonparametric maximum likelihood, etc. To construct a computationally efficient generator function, we also propose a novel form of neural network called the *weight multiplicative multilayer perceptron* to achieve fast convergence. Our numerical results demonstrate that the new neural network structure enjoys a few orders of magnitude speed advantage in comparison to the conventional one. An R package called GMS is provided, which runs under `PyTorch` to implement the proposed methods and allows the user to provide a customized loss function to tailor to their own models of interest.

## 1 Introduction

Consider a canonical statistical model in which  $\mathbf{y} = \{y_1, \dots, y_n\}$  are i.i.d. observations following a statistical model with the parameter of interest denoted by  $\theta \in \Theta \subset \mathbb{R}^p$ . In some instances such as regression, one may also include predictors or covariate variables for each observation. An efficient estimator of  $\theta$  can often be found by solving the following (penalized) optimization problem:

$$\hat{\theta} = \underset{\theta}{\operatorname{argmin}} L_{\mathbf{y}}(\theta), \quad \text{with } L_{\mathbf{y}}(\theta) \equiv \frac{1}{n} \sum_{i=1}^n \ell_{\eta}(\theta; y_i),$$

where  $\ell_\eta(\cdot)$  is a suitable loss function chosen by the researcher. The resulting  $\hat{\theta}$  is often referred to as an *M-estimator* (Huber, 1992). For example, the maximum likelihood estimator is a special M-estimator.

To assess the variability of the M-estimator  $\hat{\theta}$ , we study behaviors of the following *tunable weighted M-estimators* as inspired by the bootstrap methods (Efron, 1979; Newton and Raftery, 1994):

$$\hat{\theta}_{\mathbf{w},\lambda,\eta} = \underset{\theta}{\operatorname{argmin}} L_{\mathbf{y}}(\theta; \mathbf{w}, \lambda, \eta), \quad \text{with } L_{\mathbf{y}}(\theta; \mathbf{w}, \lambda, \eta) \equiv \frac{1}{n} \sum_{i=1}^n w_i \ell_\eta(\theta; y_i) + \lambda u(\theta), \quad (1)$$

where  $\eta \in \mathbb{R}^+$  is an auxiliary parameter of the loss,  $u(\cdot)$  is a penalty function on the parameter with a tuning parameter  $\lambda$  that can be set to zero for non-penalized settings, and  $\mathbf{w} = (w_1, \dots, w_n)^\top \in \mathcal{W}$  is a vector of weights following distribution  $\pi(\mathbf{w})$ . The auxiliary parameter  $\eta$  tunes the loss function. For example, in quantile regression models,  $\eta \in (0, 1)$  represents the quantile level and the loss function takes the form

$$\ell_\eta(\theta; y_i, X_i) := \rho_\eta(y_i - X_i^\top \theta), \quad \text{where } \rho_\eta(t) = t(\eta - I(t < 0)).$$

When the loss function has no auxiliary parameter, we simply denote the loss and the resulting estimator by  $\ell(\theta; y_i)$  and  $\hat{\theta}_{\mathbf{w},\lambda}$ , respectively.

The formulation of (1) applies to a wide range of statistical procedures. For example, the classical bootstrap procedure of Efron (1979) corresponds to  $u(\theta) = 0$  and  $\pi(\mathbf{w}) = \text{Multinom}(\mathbf{w}; n, \mathbb{1}_n/n)$ , where  $\mathbb{1}_n$  is a  $n$ -dimensional vector of one. The random-weight bootstrap can be formulated by imposing a general distribution on  $\mathbf{w}$  that has a mean of one and a variance of one. Their theoretical properties such as consistency have been studied (Præstgaard and Wellner, 1993; Cheng and Huang, 2010; Giné and Zinn, 1990; Barbe and Bertail, 2012). A special and most well-known form of the random-weight bootstrap is to set  $\mathbf{w} \sim n \times \text{Dirichlet}(n; \mathbb{1}_n)$  as in *Bayesian Bootstrap* (Rubin, 1981) and *Weighted Likelihood Bootstrap* (Newton and Raftery, 1994). Theoretical investigations and improvements of the bootstrap methods have been considered in a large body of literature (Chatterjee et al., 2005; McCarthy et al., 2018; Hall and Martin, 1988; Efron, 1987; Hahn, 1995; Bühlmann, 2002; Kleiner et al., 2014).

Iterated bootstrap procedures are often employed to reduce the bias associated with a statistical inference procedure and/or improve the coverage precision of confidence intervals (Hall and Martin, 1988). A most frequently cited procedure is the double bootstrap, which first bootstraps and infers the parameter or prediction, and then estimates the bias of each bootstrapped solution via a second-level bootstrap. In (1), the double bootstrap procedures can be represented by setting a hierarchical weight distribution such that  $\mathbf{s} = \{s_1, \dots, s_n\} \sim \text{Multinom}(n, \mathbb{1}_n/n)$  and  $\mathbf{w} \mid \mathbf{s} \sim \text{Multinom}(n, \mathbf{s}/n)$ . These iterated bootstrap methods can be shown to provide more accurate corrections (i.e., the second or higher-order accuracy), compared with single bootstraps and asymptotic approximations

(Martin, 1992; McCarthy et al., 2018; Hall, 2013; Lee and Young, 1999, 1995). However, iterative bootstraps are computationally very expensive and are seldom practically used when the data are of moderate to large size.

The tunable weighted M-estimation in (1) can also represent  $K$ -fold cross-validation. For pre-selected folds, such as a group of sample indices  $I_1, \dots, I_K$ , we set  $w_i = 0$  for  $i$  in the fold of interest, say  $I_1$ , and set  $w_i = 1$  in all other folds. This means that the observations in  $I_1$  will be ignored during training, rendering  $I_1$  to be test samples. If  $u(\cdot) = \|\cdot\|_1$ , the evaluated  $\hat{\theta}_{\mathbf{w},\lambda}$  is equivalent to the LASSO estimator (Tibshirani, 1996), based on a tuning parameter  $\lambda$ , trained without using the samples in the considered fold  $I_1$ , resulting in a cross-validated LASSO. The computational burden of the cross-validation linearly increases with the fold size  $K$  and the candidate set size of the tuning parameter, and a typical amount is at least a few hundreds of repetitive computations.

While aforementioned weighted M-estimation procedures are widely used in statistics and science, the computational bottleneck caused by their repetitive nature poses significant practical difficulties. To alleviate these computational difficulties, we propose a computational strategy based on a generative process modelled by a neural network (NN), called the *Generative Multi-purpose Sampler* (GMS) (with the *Generative Bootstrap Sampler* (GBS) as a special case for bootstrap). Instead of repeating the same optimization process for various combinations of weights  $\mathbf{w}$ 's and parameters  $\lambda$ 's and  $\eta$ 's, the GMS constructs a generator function that takes  $(\mathbf{w}, \lambda, \eta)$  as input, and returns the corresponding weighted M-estimator  $\hat{\theta}_{\mathbf{w},\lambda,\eta}$ . In addition to taking advantage of the high representation power of neural networks, a key idea for the GMS to achieve the desired computational efficiency gain is to minimize an integrative loss in the training of GMS, which optimizes both the M-estimation and the parameters employed by the GMS simultaneously.

The rest of the article is organized as follows. Section 1 introduces the general GMS framework and uses a toy example to explain its potential gains. Section 3 details its specialization for the bootstrap, namely the *generated bootstrap sampler* (GBS). Section 4 discusses the training of GMS for cross-validation with Lasso and quantile regression. Section 5 explores the application of GMS for bootstrapping nonparametric MLE for hierarchical models. Section 6 provides details on the neural network structures and training for GMS. Section 7 concludes with a brief discussion.

## 2 Generative Multi-purpose Sampler

### 2.1 The basic formulation

Here we take a new viewpoint at the weighted M-estimation by explicitly treating  $\hat{\theta}_{\mathbf{w},\lambda,\eta}$  as a function of the weight  $\mathbf{w}$ , the tuning parameter  $\lambda$ , and the auxiliary parameter  $\eta$ , i.e.,  $G(\mathbf{w}, \lambda, \eta)$ , which can be approximated by a member in a family of functions  $\mathcal{G} = \{G_\phi :$

$\mathbb{R}^{n+1+1} \mapsto \mathbb{R}^p, \phi \in \Phi\}$ , where  $\Phi$  represents the space of parameters that characterize a suitable function family. By doing so, we turn the original unrestricted optimization problem in (1) into a more restrictive optimization problem in the functional space, i.e., finding a proper parameter of the generator function such that

$$\begin{aligned}\hat{\phi} &= \operatorname{argmin}_{\phi \in \Phi} \frac{1}{n} \sum_i^n w_i \ell(G_\phi(\mathbf{w}, \lambda, \eta); y_i) + \lambda u(G_\phi(\mathbf{w}, \lambda, \eta)) \\ &\triangleq \operatorname{argmin}_{\phi \in \Phi} L_{\mathbf{y}}(G_\phi(\mathbf{w}, \lambda, \eta); \mathbf{w}, \lambda, \eta),\end{aligned}\quad (2)$$

for all  $\mathbf{w} \in \mathcal{W}$ ,  $\lambda \in \mathbb{R}^+$ , and  $\eta \in \mathbb{R}^+$ .

A slightly less ambitious, but more robust and practically almost equivalent, formulation is to solve

$$\hat{\phi} = \operatorname{argmin}_{\phi \in \Phi} \mathbb{E}_{\mathbf{w}, \lambda, \eta} [L_{\mathbf{y}}(G_\phi(\mathbf{w}, \lambda, \eta); \mathbf{w}, \lambda, \eta)], \quad (3)$$

where  $\mathbb{E}_{\mathbf{w}, \lambda, \eta}(\cdot)$  is taken with respect to a proper distribution of  $(\mathbf{w}, \lambda, \eta)$  defined on  $\mathcal{W} \times \mathbb{R}^+ \times \mathbb{R}^+$ . We name this generative framework in (3) as the GMS. For non-penalized settings without the auxiliary parameter  $\eta$ , we simply denote the generator function by  $G(\mathbf{w})$ . We also use the notation  $\hat{G} = G_{\hat{\phi}}$ .

For bootstrap applications, we can appropriately choose the weight distribution. The weight distribution for Efron's nonparametric bootstrap is simply  $\mathbf{w} \sim \text{Multinom}(n, \mathbb{1}_n/n)$ . For Bayesian bootstrap (Rubin, 1981),  $\pi(\mathbf{w})$  can be set as  $n \times \text{Dirichlet}(n, \mathbb{1}_n)$ . The distributions of  $\lambda$  and  $\eta$  can simply be the uniform distribution on candidate sets of  $\lambda$ 's and  $\eta$ 's chosen by the researcher. Another reasonable distribution of  $\lambda$  and  $\eta$  is to add random noises to the candidate values (see Section 6.3 for details). The following theorem formally states that the generated estimator  $\hat{G}(\mathbf{w}, \lambda, \eta)$  is equivalent to the solution of the standard weighted M-estimator based on  $\{\mathbf{w}, \lambda, \eta\}$ , provided that the family  $\mathcal{G}$  is large enough.

**Theorem 2.1.** *Suppose that  $\hat{\phi}$  is the solution of (3) for a sufficiently large family  $\mathcal{G}$  and a proper distribution on  $\{\mathbf{w}, \lambda, \eta\}$ ,  $\mathbb{P}_{\mathbf{w}, \lambda, \eta}$ , supports  $\mathcal{W} \times \mathbb{R}^+ \times \mathbb{R}^+$ . Consider the solution of (1),  $\hat{\theta}_{\mathbf{w}, \lambda, \eta}$ , assuming its uniqueness for any given  $\mathbf{w} \in \mathcal{W}$ ,  $\lambda \geq 0$ , and  $\eta \geq 0$ . Then,  $G_{\hat{\phi}}(\mathbf{w}, \lambda, \eta) = \hat{\theta}_{\mathbf{w}, \lambda, \eta}$  almost surely in  $\mathbb{P}_{\mathbf{w}, \lambda, \eta}$ .*

*Proof.* For a given  $\mathbf{w} \geq 0$ ,  $\lambda \geq 0$ , and  $\eta \geq 0$ , we have  $L_{\mathbf{y}}(\theta; \mathbf{w}, \lambda, \eta) \geq L_{\mathbf{y}}(\hat{\theta}_{\mathbf{w}, \lambda, \eta}; \mathbf{w}, \lambda, \eta)$ , which implies  $\sum_{i=1}^n w_i \ell_\eta(\theta; y_i) + \lambda u(\theta) \geq \sum_{i=1}^n w_i \ell_\eta(\hat{\theta}_{\mathbf{w}, \lambda, \eta}; y_i) + \lambda u(\hat{\theta}_{\mathbf{w}, \lambda, \eta})$  for all  $\theta \in \Theta$ , which means that

$$\mathbb{E}_{\mathbf{w}, \lambda, \eta} \left[ L_{\mathbf{y}}(G_{\hat{\phi}}(\mathbf{w}, \lambda, \eta); \mathbf{w}, \lambda, \eta) \right] \equiv \mathbb{E}_{\mathbf{w}, \lambda, \eta} \left[ L_{\mathbf{y}}(\hat{\theta}_{\mathbf{w}, \lambda, \eta}; \mathbf{w}, \lambda, \eta) \right].$$

because the solution  $\hat{\theta}_{\mathbf{w}, \lambda, \eta}$  is unique for any given  $\mathbf{w}$ ,  $\lambda$ , and  $\eta$ ,  $G_{\hat{\phi}}(\mathbf{w}, \lambda, \eta)$  must be equal to  $\hat{\theta}_{\mathbf{w}, \lambda, \eta}$  for almost all  $\mathbf{w}$ ,  $\lambda$ , and  $\eta$  under the probability measure  $\mathbb{P}_{\mathbf{w}, \lambda, \eta}$ .  $\square$

Of course, this nearly trivial theorem has no immediate practical application since the function family  $\mathcal{G}$  is not specified. It does, however, suggest that optimizing the integrative loss over the space of  $(\mathbf{w}, \lambda, \eta)$  instead of the individual loss can be an attractive choice. Thus, to benefit from this formulation, we must choose an appropriate family  $\mathcal{G}$  of functions  $G_\phi$  and a suitable distribution  $\mathbb{P}_{\mathbf{w}, \lambda, \eta}$  to cover the weight-hyperparameter space of interest. As demonstrated by our empirical studies on a wide range of problems, restricting  $\mathcal{G}$  to be a class of neural networks and choosing a reasonable distribution  $\mathbb{P}_{\mathbf{w}, \lambda, \eta}$  appears to work well (see details in Section 6.3).

As shown in Cybenko (1989); Lu et al. (2017), *Multi-Layer Perceptrons* (MLP), or equivalently, *feed-forward neural networks* (FNNs), are theoretically capable of approximating any Lebesgue integrable function when the numbers of neurons and layers are sufficiently large. Also, recent successful applications of deep neural networks in a variety of data-rich fields provide compelling evidence supporting the use of over-parameterized MLPs and other types of NNs for approximating extremely complicated functions (Goodfellow et al., 2014; Arjovsky et al., 2017; Isola et al., 2017). With the adoption of MLPs, the optimization task in (3) is to minimize the loss function with respect to the parameters of the neural network, which can be implemented via a *backpropagation* algorithm (Rumelhart et al., 1986) along with the *Stochastic Gradient Descent* (SGD) algorithm and its variants. These operations can be numerically carried out via an efficient GPU-accelerated platform such as `pytorch` and `tensorflow`. The details of the employed neural networks are given in Section 6.1.

## 2.2 Intuitions for potential gains

Imagine that we have independent weight vectors  $(\mathbf{w}^{(1)}, \lambda^{(1)}, \eta^{(1)}), \dots, (\mathbf{w}^{(M)}, \lambda^{(M)}, \eta^{(M)})$  from  $\mathbb{P}_{\mathbf{w}, \lambda, \eta}$ , we can approximate the expectation in (3) by

$$\mathbb{E}_{\mathbf{w}, \lambda, \eta} [L_{\mathbf{y}}(G(\mathbf{w}, \lambda, \eta); \mathbf{w}, \lambda, \eta)] \approx \frac{1}{M} \sum_{m=1}^M L_{\mathbf{y}}(G(\mathbf{w}^{(m)}, \lambda^{(m)}); \mathbf{w}^{(m)}, \lambda^{(m)}, \eta^{(m)}), \quad (4)$$

and new samples of  $\mathbf{w}$ ,  $\lambda$ , and  $\eta$  can be generated within the iterative algorithm so that a small size  $M$  should work well, say  $M = 100$ . An intuition for this is that the two optimization problems in fact help each other: a stochastic gradient move that changes  $G$  in (4) is re-evaluated with a modified set of weights; and the objective function  $\ell(\cdot)$  and the generator  $G(\cdot)$  co-evolve to achieve the minimum.

If we were to cast the task of training a generator in a classical machine learning framework, we would have to first obtain a set of training samples,  $\{(\mathbf{w}^{(b)}, \lambda^{(b)}, \hat{\theta}^{(b)})\}_{b=1}^B$ , where  $\hat{\theta}^{(b)} = \hat{\theta}_{\mathbf{w}^{(b)}, \lambda^{(b)}}$ , by evaluating  $B$  optimizations in (1) with  $(\mathbf{w}^{(b)}, \lambda^{(b)})$  for  $b = 1, \dots, B$  (ignoring  $\eta$  for simplicity in this case). Then, one may try to learn a function  $g$

by minimizing

$$\hat{g} = \underset{g}{\operatorname{argmin}} \sum_{b=1}^B \|\hat{\theta}^{(b)} - g(\mathbf{w}^{(b)}, \lambda^{(b)})\|^2, \quad (5)$$

under the  $l_2$ -distance  $\|\cdot\|$ . However, this squared-loss measures the distance between the fitted generator  $\hat{g}(\mathbf{w}, \lambda)$  and its observed true value  $\hat{\theta}_{\mathbf{w}, \lambda}$ . As a result, it cannot inform us how to improve the fitting of the original statistical loss in (1) other than a simple interpolation. Thus, the function trained in this manner tends to be inaccurate if  $B$  is small, or may be prohibitively expensive in computation if we must rely on a large  $B$ . Additionally, if an excessive number of repetitive optimizations is required, the computational advantage of the generative procedure would be non-existing or limited.

In comparison, training the generator function  $G$  in conjunction with minimizing the loss function via the GMS formulation (3) is significantly more efficient. The classical loss (5) fits only on the training data with a limited size,  $\{(\mathbf{w}^{(b)}, \lambda^{(b)}, \hat{\theta}^{(b)})\}_{b=1}^B$ , resulting in an over-fitting issue. The GMS, on the other hand, is trained using the weights and tuning parameters generated from a predefined distribution without requiring additional optimizations for (1), and generating  $\mathbf{w}$  and  $\lambda$  is nearly cost-less. As a result, the GMS training procedure not only seeks the minimizer of  $L_{\mathbf{y}}(\theta; \mathbf{w}, \lambda)$ , but also allows for the use of an almost infinite number of training weights and tuning parameters during the training step, thereby avoiding over-fitting.

### 2.3 Illustration with a simple example

A novel aspect of our new formulation is represented by the minimization of the integrative loss (3), which combines the individual optimization step required by each classical replication with the approximation of the functional form  $G$ . Let us consider the bootstrap procedure for a toy linear regression example with data  $(y_i, X_i)$ ,  $i = 1, \dots, n$ , and the loss function  $l(\theta; y_i, X_i) = (y_i - X_i^\top \theta)^2$  and  $\lambda = 0$ . For this problem, we can obtain the closed-form solution of the optimization problem for each bootstrapped sample:  $G_0(\mathbf{w}) = (\mathbf{X}^\top W \mathbf{X})^{-1} \mathbf{X}^\top W \mathbf{y}$ , where  $\mathbf{y} = (y_1, \dots, y_n)^\top$ ,  $\mathbf{X} = (X_1^\top, \dots, X_n^\top)^\top$ , and  $W = \operatorname{diag}(\mathbf{w})$  is a diagonal matrix. Thus, a bootstrap procedure would follow simple steps: for  $b = 1, \dots, B$ , generate  $\mathbf{w}^{(b)} = (w_1^{(b)}, \dots, w_n^{(b)}) \sim \mathbb{P}_{\mathbf{w}}$ , a multinomial distribution, and then, for each  $\mathbf{w}^{(b)}$ , plug in the formula to get  $\hat{\theta}^{(b)} = G_0(\mathbf{w}^{(b)})$ . However, if one does not have the closed-form formula but has to solve numerically the minimization problem of (1) for every generated  $\mathbf{w}^{(b)}$ , the bootstrap procedure can be prohibitively demanding in computation. Thus, our GMS formulation via (3) can be thought of as an automatic way to find a highly accurate approximation to the closed-form solution (in the form of an NN) of the minimization problem of (1). Once this solution  $\hat{G}$  is found, one can easily generate bootstrap estimators with almost no computational cost.

For a case of  $n = 100$  and  $p = 10$ , we set the true coefficient  $\theta = \{1, 0, \dots, 0\}$  and the

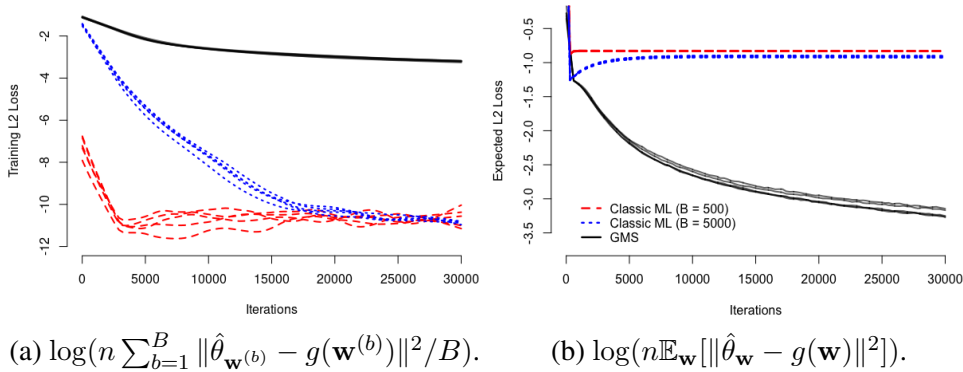


Figure 1: Trace plots of the training loss (a) and the integrative prediction loss (b) in logarithmic scales. Five lines for each optimization represent five distinct initializations; and the red dashed and blue dotted lines indicate the conventional ML training method with  $B = 500$  and  $B = 5,000$ , respectively.

regression variance one. The predictors are independently generated from  $N(0, I_p)$ . Even though this example is simple, constructing the generator function is non-trivial, because the generator function’s input dimension is 100, and the dimension of its codomain is 10. Training a 100-dimensional function with 10-dimensional codomain requires a large number of training samples in the framework of (5). This fact is reiterated in Figure 1. We generate a data set and evaluate random weight bootstrap estimators with  $\mathbf{w} \sim n \times \text{Dirichlet}(n; 1, \dots, 1)$ , and then numerically evaluate the average loss of (1) on various weights from the trained generator for the classical machine learning approach with  $B = 500$  and  $B = 5,000$ , as well as the GMS. We initialize the optimization in different five points for each procedure. Their loss values are tracked and illustrated in Figure 1.

We consider two performance measures for this example: the training loss specified in (5) and the integrative predictive loss  $\mathbb{E}_{\mathbf{w}}[\|\hat{\theta}_{\mathbf{w}} - g(\mathbf{w})\|^2]$ . The integrative prediction loss is approximated by using 1,000,000 bootstrap evaluations, and the loss values are multiplied by  $n$  to adjust for the scale of  $\text{var}(\hat{\theta})$ . Note that the GMS generator  $G$  is trained by minimizing the integrative loss (3), whereas the naive generator  $g$  is trained using the  $l_2$ -loss in (5) with training sizes  $B = 500$  and  $5,000$ , respectively. As expected, Figure 1 (a) shows that the training  $l_2$ -losses for the naive procedures are significantly less than those for the GMS. However, the integrative predictive losses (IPL) behave quite differently. The naive minimizers (trained with  $B = 500$  and  $B = 5,000$  training samples, respectively) first decrease their IPLs rapidly, but after 200 iterations their IPLs begin to increase. In contrast, the GMS to seamlessly reduces its IPL, converging to the target quantity. This suboptimal performance of the naive procedure stems from the fact that the  $l_2$ -loss encourages the generator function  $\hat{g}$  to overfit to the training data set  $\hat{\theta}^{(1)}, \dots, \hat{\theta}^{(B)}$ . Unlike the conventional machine learning modeling, the GMS is quite resistant to overfitting, as we can sample  $\mathbf{w}$ ’s at near-zero computational cost. Figure 1 demonstrates that the GMS optimization behavior is very stable for both the training and integrative predictive losses.

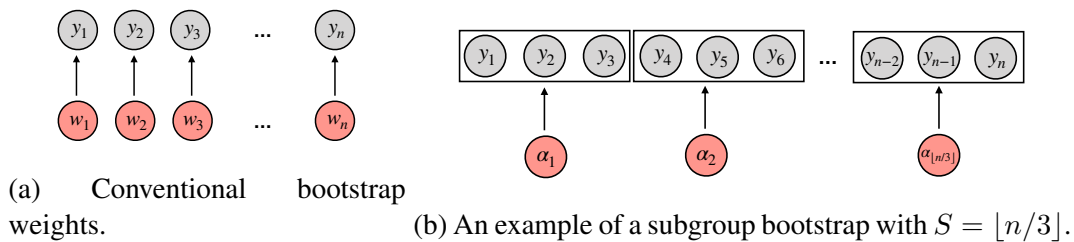


Figure 2: The structure of bootstrap weights for the subgroup bootstrap.

### 3 Generative Bootstrap Samplers

The simplest use of the GMS is to bootstrap M-estimators, which is a special case of form (3) without  $\eta$  and  $u(\cdot)$ , employing a bootstrap weight distribution  $\text{Multinom}(n, \mathbb{1}_n/n)$  (or  $n \times \text{Dirichlet}(n, \mathbb{1}_n)$  for Bayesian bootstrap). More precisely, we let  $\phi$  be the parameter underlying the generator  $G$  and solve the optimization problem:

$$\hat{\phi} = \underset{\phi \in \Phi}{\operatorname{argmin}} \mathbb{E}_{\mathbf{w}} \left[ \frac{1}{n} \sum_{i=1}^n w_i \ell(G_{\phi}(\mathbf{w}); y_i) \right].$$

3 We call this simple GMS application *Generative Bootstrap Sampler* (GBS). In this section, we will explore the details of the GBS applications in various bootstrap procedures.

#### 3.1 Bootstrap and subgroup bootstrap

Despite its considerable efficiency, the GBS framework has a fundamental limitation for practical bootstrap applications: the dimension of the generator domain equals the sample size  $n$ . Even when computationally efficient neural networks are used to model the generator, the optimization convergence of the model is quite slow when the input dimension is high (say, tens of thousands). We may further encounter technical issues such as memory shortage as well, which is particularly severe for big data. To address this limitation, we consider a subgroup weighting, which divides the data set into subgroups and assigns equal weights to observations within each subgroup. This concept of subgrouping is primarily used for bootstrapping time series data sets, referred to as *block bootstrap* (Lahiri, 1999; Härdle et al., 2003), in order to preserve the temporal association within bootstrapped samples. In contrast to the time series applications, we use subgrouping (or blocking) to reduce the number of weights, or more precisely, the domain dimension of the generator function so as to save computational costs.

Let  $[n]$  denote the index set  $\{1, \dots, n\}$  of the observations. We consider a partition:  $I_1, \dots, I_S \subset [n]$  such that  $I_i \cap I_j = \emptyset, \forall i \neq j$ , and  $\cup_{s=1}^S I_s = [n]$ . Without loss of generality, we assume that the size of each  $I_s$  is the same, i.e.,  $|I_s| = n/S$  for  $s = 1, \dots, S$ . We define an subgroup assignment function  $h : [n] \mapsto [S]$  such that  $h(i) = s$  if  $i \in I_s$ . Then, for  $\{\alpha_1, \dots, \alpha_S\}^T \sim \mathbb{P}_{\alpha}$ , with  $\mathbb{P}_{\alpha}$  being an  $S$ -dimensional weight distribution, we



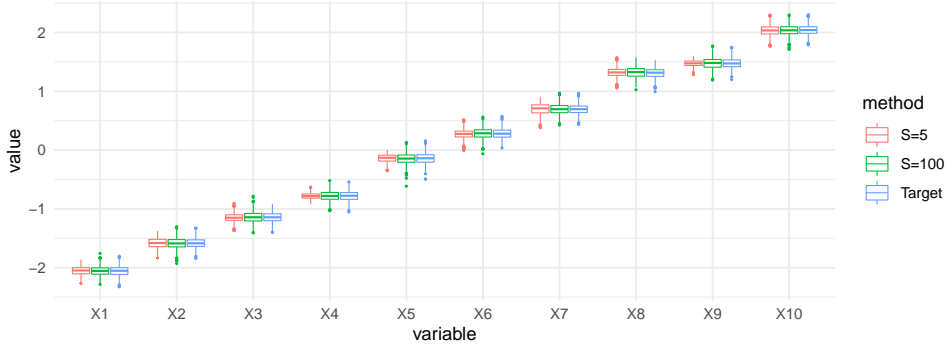


Figure 3: Comparisons of subgroup bootstraps across different numbers of blocks.

impose the same value of weight on all elements in a subgroup as

$$w_i = \alpha_{h(i)} \quad \text{for } i = 1, \dots, n. \quad (6)$$

and we denote  $\mathbf{w}_\alpha = \{\alpha_{h(1)}, \dots, \alpha_{h(n)}\}^\top \in \mathbb{R}^n$ . As a result, it follows that  $\alpha_{h(i)} = \alpha_{h(k)}$ , if  $i, k \in I_s$  for some  $s$ . Similar to the vanilla GBS previously introduced, setting  $\alpha \sim \text{Multinomial}(S, \mathbb{1}_S/S)$  and  $\alpha \sim S \times \text{Dirichlet}(S, \mathbb{1}_S)$  result in the block-based nonparametric bootstrap and Bayesian bootstrap, respectively. For technical convenience, we rewrite the weight assignment (6) as a linear transformation:  $\mathbf{w}_\alpha = Q\alpha$ , where  $Q = \{R_1, \dots, R_S\}$  and  $R_s$  is a  $n$ -dimensional vector whose  $i$ -th element is one if  $i \in I_s$  and zero otherwise, for  $s = 1, \dots, S$ . Then, each weight in  $\alpha$  is replicated at least  $\lfloor n/S \rfloor$  times in  $\mathbf{w}_\alpha = Q\alpha$ , and the reduced weights can be easily reconstructed into the original dimension by this matrix multiplication.

As an illustration, we consider a simple linear regression example by generating a data set from the model with  $n = 1000$ ,  $p = 10$ , its coefficients being a sequence of equi-spaced values between -2 and 2, and  $\sigma^2 = 2$ . Each covariate is drawn i.i.d. from  $N(0, 1)$ , and the regression variance is set to one. The resulting domain dimension of a vanilla  $G$  is 1000. When we use 100 subgroups (10 observations in each subgroup), the input dimension is reduced to 100 from the original 1000 but the resulting bootstrap confidence intervals (CIs) are nearly identical to those from the standard bootstrap (Figure reffig:block). Even when the number of subgroups is tiny ( $S = 5$ ), the obtained CIs are acceptable. This result is further confirmed by Figure 4, which shows individual histograms of bootstrap distributions with varying subgroup sizes. While the location of the subgroup bootstrap distribution is close to that of the target one for  $S = 5$ , the variability tends to be underestimated. As  $S$  increases, the quality of the approximation of the subgroup bootstrap distribution improves significantly. When  $S = 100$ , the subgroup bootstrap distributions are indistinguishable from the target ones. Not only for this toy example, in all applications we have examined, we observe that the subgroup bootstrap with  $S = 100$  is sufficiently accurate. We thus set subgroup bootstrap with  $S = 100$  as a default of the GBS (and GMS) henceforth.

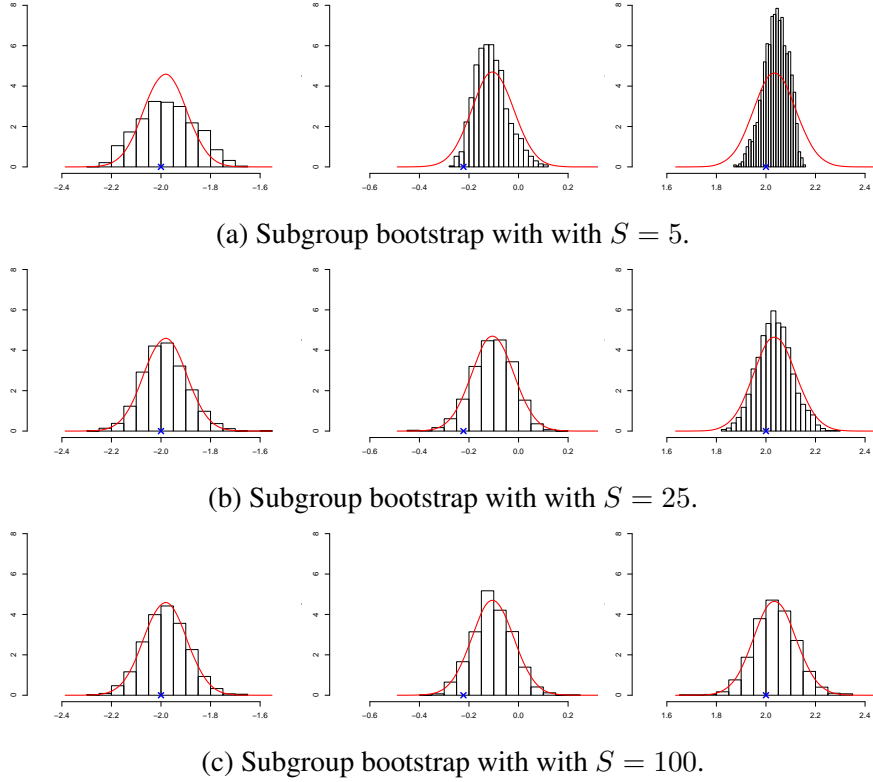


Figure 4: Histograms of block bootstrap distributions with various  $S$  for the coefficient of  $X_1$  (left column),  $X_5$  (middle column), and  $X_{10}$  (right column). The red line indicates the density function of the target distribution (of the standard bootstrap). Each true coefficient is marked by a blue  $\times$ .

More details on the theoretical justification of subgroup bootstrap can be found in the Appendix. One remark is that under some regularity conditions, the subgroup bootstrap consistency can be achieved when  $S$  is of a higher order than  $\sqrt{n}$ . This fact implies that even though setting  $S = 100$  empirically performs well, a larger subgroup size can be considered for excessively large data sets.

### 3.2 Iterated bootstrap

The iterated bootstrap method was proposed to improve the inference accuracy of the simple bootstrap method, and was shown both theoretically and empirically to achieve a higher-order accuracy for the coverage of the constructed confidence intervals and bias-corrections (Martin, 1992; McCarthy et al., 2018; Hall, 2013; Lee and Young, 1999, 1995). More precisely, an iterated bootstrap procedure involves nested levels of data resampling. Let us consider the simplest one: the double bootstrap. The double bootstrap as depicted in Figure 5 first creates  $B$  bootstrap samples,  $\mathbf{y}_b^*$ ,  $b = 1, \dots, B$  by resampling from the original data set, and then, for each bootstrapped sample  $\mathbf{y}_b^*$ , creates  $C$  second-level bootstrap samples,  $\mathbf{y}_{bc}^{**}$ ,  $c = 1, \dots, C$ , by resampling from  $\mathbf{y}_b^*$ . For each  $\mathbf{y}_b^*$  and  $\mathbf{y}_{bc}^{**}$ , we denote the corresponding estimator of  $\theta$  by  $\hat{\theta}_b^*$  and  $\hat{\theta}_{bc}^{**}$ , respectively. By iterating this

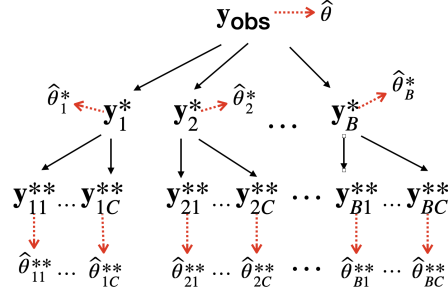


Figure 5: Double bootstrap resampling and estimates.

step, we can simply extend this to more iterated bootstrap cases.

An extension of the GBS to iterated bootstraps is immediate, as it is a special case of (3) with a weight distribution that has a hierarchical structure. For a  $d$ -level iterated bootstrap procedure, we may characterize its weight distribution hierarchically:

$$\mathbf{w}_{(1)} \sim \text{Multinom} \left( n, \frac{\mathbb{1}_n}{n} \right), \mathbf{w}_{(2)} | \mathbf{w}_{(1)} \sim \text{Multinom} \left( n, \frac{\mathbf{w}_{(1)}}{n} \right), \dots, \mathbf{w}_{(d)} | \mathbf{w}_{(d-1)} \sim \text{Multinom} \left( n, \frac{\mathbf{w}_{(d-1)}}{n} \right)$$

The computational advantage of the GBS framework is particularly significant in these situations.

**Iterated Bootstrap for Better Confidence Intervals.** Various procedures for constructing confidence intervals using bootstrap have been proposed, such as the *percentile* method (Hall, 1992), the *studentized* method (Hall, 1988; Efron, 1979), the *Bias-Corrected and accelerated* method  $BC_a$  (Efron, 1987), and *Approximated Bias Correction* (ABC; Diccio and Efron (1992)), etc. Even though  $BC_a$  and ABC procedures enjoy the second-order accuracy (fast convergence in coverage error), a practical implementation of these procedures are not trivial since it is difficult to calculate their acceleration factor for general models. On the other hand, the percentile procedure is only first-order correct, and the studentized procedure requires an iterated bootstrap, unless an explicit form of the standard error of the bootstrap estimator is available, which is computationally too expensive in a conventional bootstrap framework.

To improve the quality of the constructed CI (both the coverage accuracy and the length of the interval), we consider using double bootstraps as in the coverage calibration method (Hall and Martin, 1988; Hall, 1986) and studentized CI procedure (Hall, 1988). The calibrated percentile CIs via double bootstrap achieves the second-order accuracy ( $O(1/n)$ ) for the two-sided CI, but the single-bootstrapped counterpart has a coverage error rate of order of  $O(1/\sqrt{n})$ . Despite these advantages, applying the conventional double bootstrap requires undesirably intensive computation: a total of  $B \times C$  evaluations of bootstrap estimators  $\hat{\theta}_{bc}^{**}$  for  $b = 1, \dots, B$  and  $c = 1, \dots, C$ . Lee and Young (1999) showed that  $B$  and  $C$  should be of higher order than  $n^4$  and  $n^2$  in the two-sided case, and of order  $n^2$  and  $n$  in the one-sided case, respectively, to ensure that the coverage error

rate of the Monte Carlo interval remains equal to that of the theoretical double bootstrap interval. The authors considered  $B = 1000$  and  $C = 500$  in their simulated experiments, resulting in a total of 500,000 evaluations. This scale of computation would be infeasible with the conventional bootstrap framework in practice. In contrast, after the generator function has been trained for the GBS, it takes just tens of seconds to generate millions of bootstrap estimators, achieving a manageable computing scale for iterated bootstraps.

### 3.3 GBS for iterated bootstrap

One drawback of the standard nonparametric bootstrap is that each bootstrap sample only touches upon about  $1 - e^{-1} \approx 63\%$  of the observations due to the nature of multinomial sampling, which appears to be somewhat wasteful. This loss is compounded and become more significant in iterated bootstraps. A smoothed version of these weight distributions is a hierarchy of Dirichlet distributions, which enable each  $\hat{\theta}_b^*$  and  $\hat{\theta}_{bc}^*$  to utilize all the observations (Cheng and Huang, 2010; Xu et al., 2020; Præstgaard and Wellner, 1993). Thus, we consider that  $\mathbf{w} \mid \mathbf{z} \sim n \times \text{Dirichlet}(n, \mathbf{z})$  and  $\mathbf{z} \sim n \times \text{Dirichlet}(n, \mathbb{1}_n)$ . If subgroup bootstrap as introduced in Section 3.1, is employed the subgrouped weights follow  $\mathbf{w} \mid \mathbf{z} \sim S \times \text{Dirichlet}(S, \mathbf{z})$  and  $\mathbf{z} \sim S \times \text{Dirichlet}(S, \mathbb{1}_S)$ . We can train a generator function that covers both single and double bootstraps by adopting a probabilistic mixture of single and double bootstrap weights distributions; e.g., generate single or double bootstrap weights with 50%-50% chances.

### 3.4 An illustration: double-bootstrap for logistic regression

We consider the standard logistic regression model:

$$y_i \sim \text{Bernoulli} \left( \frac{1}{1 + \exp\{-X_i^T \boldsymbol{\theta}\}} \right), \quad \text{where } X_i \in \mathbb{R}^p, \boldsymbol{\theta} = (\theta_1, \dots, \theta_p)^T, i = 1, \dots, n.$$

To apply the GBS to this model, we simply set

$$\ell(\boldsymbol{\theta}; y_i) = (1 - y_i) \log X_i^T \boldsymbol{\theta} + \log(1 + \exp(-X_i^T \boldsymbol{\theta}))$$

in (3). We simulate a data set that contains  $n = 400$  observations, each with  $p = 20$  covariates generated independently from the standard Gaussian. The true coefficients  $\theta_j = 0.631(j - 10.5)$  for  $j = 1, \dots, 20$  (an equi-spaced sequence between  $-6$  and  $6$ ).

We examine 95% CIs constructed by various procedures, including a bias-corrected percentile CI (single bootstrap, called the “basic”), a BCa CI (Efron, 1987), a calibrated percentile CI (double bootstrap), and a studentized CI (double bootstrap). The “basic” CI is constructed as  $(2\hat{\theta} - q_{97.5\%}^*, 2\hat{\theta} - q_{2.5\%}^*)$ , where  $q_\beta^*$  is the  $\beta$ -quantile of the bootstrap distribution of  $\hat{\theta}^*$ . The calibrated percentile CI is obtained as  $(2\hat{\theta} - q_{\hat{\alpha}_U}^*, 2\hat{\theta} - q_{\hat{\alpha}_L}^*)$ , where  $\hat{\alpha}_L$  and  $\hat{\alpha}_U$  are calibrated coverage levels via the double bootstrap aiming at 2.5% and

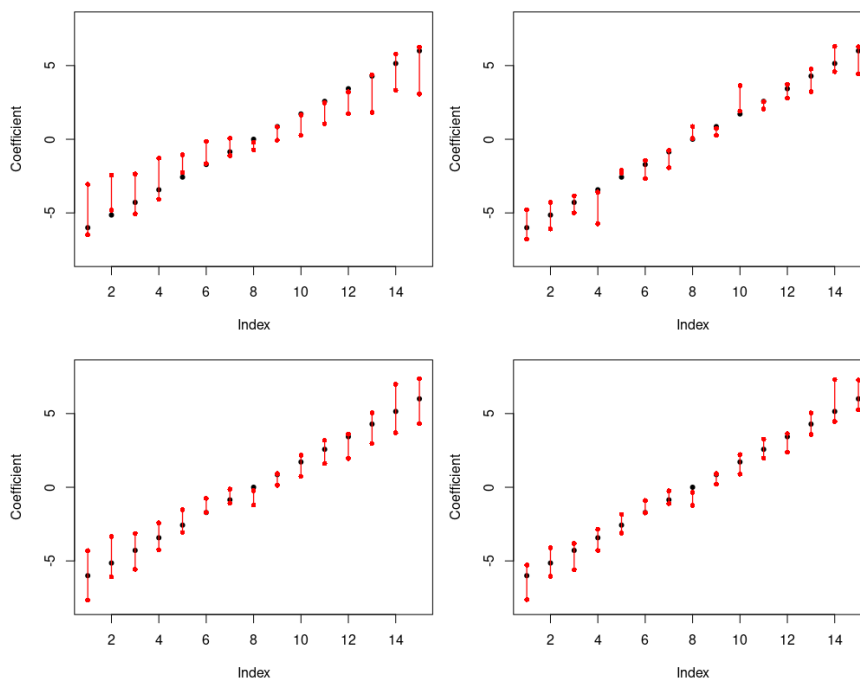


Figure 6: 95% CIs for the logistic regression example: The basic single bootstrap CI (top left); the BCa CI (top right); the calibrated percentile bootstrap CI via double bootstrap (bottom left); a studentized bootstrap CI via double bootstrap (bottom right). True parameter values are marked by black dots.

97.5%, respectively. The studentized CI is  $(\hat{\theta} - \tilde{t}_{97.5\%}^* \hat{s}, \hat{\theta} - \tilde{t}_{2.5\%}^* \hat{s})$ , where  $\tilde{t}_{\beta}^*$  is the  $\beta$ -quantile of the studentized bootstrap statistic, and  $\hat{s}$  is the estimated standard error. The detailed descriptions of these bootstrap procedures, as well as the notation, are given in the Appendix.

For the double bootstrapped CIs, we consider 5000 bootstrap estimators for the first-level bootstrap and 1000 for the second-level, resulting in a total of  $5000 \times 1000 = 5,000,000$  bootstrap evaluations. This poses a significant computational challenge under the conventional framework. In comparison, once trained (which takes less than 3 minutes for this example), the GBS produces 10,000 bootstrap estimators in less than 1 second. The GBS' computational advantage also applies to larger-sized data sets and more complicated models as shown below and in later sections.

### 3.5 Scaling up towards large $n$ and $p$

We consider the same logistic regression model as in the previous subsection with the true regression coefficients  $\theta_j$ 's equally spaced between -3 and 3. We compared the performance of the GBS with those of the standard bootstrap, BCa, and the profile likelihood confidence interval with sample size  $n \in \{500, 5000, 10000\}$  and dimension of covariates  $p \in \{30, 200, 300\}$ . This simulation is replicated independently 20 times. We examine properties of the 95% CIs constructed by these bootstrap methods (i.e., the average coverage and average width) their actual computing time. For standard bootstrap procedures,

Method	$(n, p) = (500, 30)$			$(n, p) = (5000, 200)$			$(n, p) = (10000, 300)$		
	Cov	Width	Time	Cov	Width	Time	Cov	Width	Time
GBS1 (Basic)	0.975	1.804	140.8 + <b>0.1</b>	0.987	1.028	152.9 + <b>0.2</b>	0.976	0.721	163.6 + <b>0.4</b>
GBS1 (Percentile)	0.752	1.804	140.8 + <b>0.1</b>	0.217	1.028	152.9 + <b>0.2</b>	0.199	0.721	163.6 + <b>0.4</b>
GBS2 (Student)	0.962	1.548	140.8 + <b>15.6</b>	0.960	0.904	152.9 + <b>45.0</b>	0.931	0.651	163.6 + <b>63.9</b>
GBS2 (Calibrated)	0.933	1.463	140.8 + <b>15.6</b>	0.954	0.894	152.9 + <b>45.0</b>	0.938	0.661	163.6 + <b>63.9</b>
Basic (25C)	1.000	1.899	8.4	1.000	1.237	539.6	NA	NA	4227.05
Basic (1C)			93.8			3833.3			25540.5
Percentile (25C)	0.760	1.899	8.4	0.230	1.237	539.6	NA	NA	4227.05
BCa (25C)	1.000	2.039	84.3	NA	NA	NA	NA	NA	NA
Profile	0.918	1.657	0.7	0.462	0.941	1310.8	NA	NA	8670.7

Table 1: Results of the simulation study for logistic regression models; “GBS1” and “GBS2” indicate single and double bootstraps implemented by the GBS, respectively; “Cov”, “Width”, and “Time” mean the averages (over 20 replicates) of the coverage, the width, and the actual computing time (seconds) of each evaluated 95% CI, respectively; for the computation time of the GBS, the black and red numbers indicate training and generation time (including post processing time for the GBS), respectively.

we consider a parallel computing environment using 25 CPU cores (Threadripper 2990WX 64 threads with 128GB RAM), as well as a single-core computation (denoted by “(25C)” and “(1C)”, respectively, in Table 1). For GBS procedures, RTX2080Ti with 11GB GPU RAM is used. The detailed setting is specified in Section 6.3. We use R package `boot` to implement conventional bootstrap procedures. The profile likelihood CI is based on an asymptotic approximation, and its computation is carried out by using the `confint` function in R. Due to the computational burden, we are unable to report simulation results of the conventional CI procedures for large sized data sets. In those cases, we only report the average computation times over two replicates of each procedure. For a single-threaded case, the computation time is calculated by evaluating 500 bootstrap estimators and multiplying 10 to it.

Table 1 compares traditional bootstrap procedures with their GBS equivalents in various settings. The GBS procedures are comparable to their conventional counterparts (“Basic” and “Percentile” in the table) in terms of coverage and width of the constructed CIs. When the data size is modest, i.e.,  $(n, p) = (500, 30)$ , the traditional bootstrap-based CIs are significantly faster to compute. However, as data size increases, the conventional bootstrap computations become prohibitively expensive, taking more than an hour for  $(n, p) = (10000, 300)$  using a parallel computation with 25 threads, and more than seven hours using a single thread. Due to its heavy computational need, BCa cannot produce meaningful results for moderately large data sets (e.g., for  $(n, p) = (5000, 200)$  and  $(10000, 300)$ ). The profile likelihood procedure (“Profile”), which is based on an asymptotic approximation of the sampling distribution, takes more than two hours and twenty minutes for the case with  $(n, p) = (10000, 300)$ . Even for the smallest data set with  $(n, p) = (500, 30)$ , the conventional double bootstrap procedures are nearly infeasible (taking more than 2.5 hours with a 25-threaded parallel computation). For larger data sets such as the setting with  $(n, p) = (10000, 300)$ , the double bootstrap would take more than

---

**Algorithm 1** A subgroup weight distribution for (bootstrapped)  $K$ -fold CV.

---

**Presetting:**

- Set a candidate set of the tuning parameter  $\{\lambda_1, \dots, \lambda_L\}$ .
- Randomly subgroup the data points into  $S$  blocks  $\{I_1, \dots, I_S\}$  as demonstrated in Section 3.1, and fix them. For simplicity, assume  $\lfloor S/K \rfloor$  to be an integer. Subgroup  $\{I_1, \dots, I_S\}$  into  $K$  folds, say  $\{I_1^*, \dots, I_K^*\}$ , where  $I_k^* = \{I_{(k-1)S/K+1}, \dots, I_{kS/K}\}$  for  $k = 1, \dots, K$  (each fold contains  $S/K$  blocks).

**Sampling:**

- Randomly select one  $k'$  from  $\{1, \dots, K\}$ , and set  $w_i = 0$  for  $i \in I_{k'}^*$ , and the other weights are set to be

$$\{w_i\}_{i \notin I_{k'}^*} \begin{cases} = 1 \text{ for an only CV,} \\ \sim (S - S/K) \times \text{Dirichlet}(S - S/K, \mathbb{1}_{S-S/K}) \\ \text{or Multinomial}(S - S/K, \mathbb{1}_{S-S/K}/(S - S/K)) \text{ for a bootstrapped CV.} \end{cases}$$


---

48 days using 25 threads. In contrast, the GBS training takes less than three minutes for all examined settings, and the generation and post-processing steps for the double bootstrap take roughly a minute. Additionally, the double-bootstrap GBS2 requires no additional time for training and only slightly more time for generating and post-processing than the single bootstrap GBS1 (about one minute for the case  $(n, p) = (10000, 300)$ ). As shown in the Table, the double-bootstrap CIs obtained by GBS2 have more accurate coverage probabilities and narrower widths than single bootstrap CIs.

## 4 Efficient Cross-validation for Parameter Tuning Via GMS

### 4.1 Cross-validation via GMS

Tuning parameter selection has been a challenging and computationally intensive task for many statistical and machine learning algorithms as one often has to consider a wide range of possible choices. We note that the GMS framework is not only applicable to bootstrap, but can also be used to expedite the computation of *Cross-Validation* (CV) procedures. It is easy to see that for a weight  $w_i = 0$ , the corresponding term in the weighted M-estimation loss function (1) is zero, which is equivalent to ignoring observation  $y_i$ . More generally, we denote  $\mathbf{w}_{(-I)} = \{w_1, \dots, w_n\}$  with  $w_i = 0$  for  $i \in I$  and  $\{w_i : i \notin I\} \sim (n - |I|) \times \text{Dirichlet}(n - |I|; \mathbb{1}_{n-|I|})$  (or simply  $w_i = 1$  for  $i \notin i$ ). Because for any  $i^* \in I$  the corresponding  $y_{i^*}$  does not involve in the loss function due to the fact  $w_{i^*} = 0$ , the index set  $I$  and  $I^c$  can be viewed as test and training data indexes, respectively. As a result, this formalization is in accordance with out-of-sample evaluations ignoring the test data set  $I$ . To train the CV generator, we can employ an intuitive weight distribution in (3) in the place of the multinomial or Dirichlet distributions for standard bootstraps, such as randomly selecting one of folds and setting the corresponding weights zero. The details are formally demonstrated in Algorithm 1.

Based on this setup, a simple modification from Algorithm 2, which will be introduced in Section 6.3, can be used to train the generator for the  $K$ -fold CV by randomly

generating  $\lambda$  from a candidate sets of  $\lambda$ . Once the generator is trained, generating CV evaluations is computationally efficient and fast (less than 1 second to generate 10,000 bootstrap samples in the previous examples), and one can easily compute the estimated out-of-sample error across different tuning parameters by alternating zero weight for each fold. For  $b = 1, \dots, B$  and a tuning parameter  $\lambda_l$  in a candidate set  $\{\lambda_1, \dots, \lambda_L\}$ , we set zero weights on a fold  $I_k^*$  for  $k = 1, \dots, K$ ; i.e.,  $w_i^{(b,k)} = 0$  for  $i \in I_k^*$ . The other weights follow the setting in Algorithm 1 for  $\{w_i^{(b,k)}\}_{i \notin I_k^*}$ . The (bootstrapped) CV estimator without considering the test set  $I_k^*$  can be evaluated as  $\hat{\theta}_{(-I_k^*), \lambda_l}^{(b)} = \widehat{G}(\mathbf{w}^{(b,k)}, \lambda_l)$ . Then, the CV error for the  $k$ -th fold follows that  $\hat{e}_l^{(b,k)} = \sum_{i \in I_k^*} \ell(\hat{\theta}_{(-I_k^*), \lambda_l}^{(b)}; y_i) / |I_k^*|$ , and we repeat this for all  $K$  folds. The resulting CV error can be evaluated as  $\bar{e}_l^{(b)} = \sum_{k=1}^K \hat{e}_l^{(b,k)} / K$  for  $b = 1, \dots, B$ .

After evaluating  $\bar{e}_l^{(b)}$  for  $l = 1, \dots, L$  and  $b = 1, \dots, B$ , one can easily identify the bootstrap distribution of the out-of-sample loss via the empirical distribution of  $\{\bar{e}_l^{(b)}\}_{b=1, \dots, B}$  under  $\lambda_l$ , as well as confidence bands of the out-of-sample loss. Moreover, with  $l^{(b)} = \arg\min_l \{\bar{e}_l^{(b)}\}$ , the empirical distribution of  $\{\lambda_{l^{(b)}}\}_{b=1, \dots, B}$  serves as the bootstrap distribution of the minimizer of CV errors and can naturally quantify the uncertainty of the chosen tuning parameter via the CV (an example is given in the left of Figure 8). Furthermore, this bootstrap distribution of the minimizer of CV errors provides an alternative of the *one-standard error rule* commonly used with CV for Lasso regression, in which we choose the most parsimonious model whose error is no more than one standard error above the error of the best model. Since the standard deviation of the CV errors cannot be estimated accurately, this procedure is often too variable. In contrast, our new procedure provides a bootstrap distribution for the minimizer of CV errors. To pursue more parsimonious tuning parameter selection, we can use the upper 90% confidence bound of this bootstrap distribution as our chosen  $\lambda$ , which appears to be more principled.

## 4.2 Cross-validation for LASSO and ridge regression

Two representative examples of the penalized M-estimation are ridge and LASSO regression models (Tibshirani, 1996), with the corresponding loss function for GMS:

$$\mathbb{E}_{\mathbf{w}, \lambda} \left[ \frac{1}{n} \sum_{i=1}^n w_i \{y_i - X_i^T G(\mathbf{w}, \lambda)\}^2 + \lambda u(G(\mathbf{w}, \lambda)) \right], \quad (7)$$

where  $u(x) = \|x\|_2^2$  for the ridge and  $u(x) = \|x\|_1$  for the LASSO. By changing the loss and the penalty part in (7), we can easily apply the GMS to other penalized M-estimators. After obtaining the trained  $\widehat{G}$  from (7), a bootstrapped evaluation from  $\mathbf{w}^*$  and  $\lambda^*$ , which minimizes  $\sum_{i=1}^n w_i^* \ell(\theta; y_i) / n + \lambda^* u(\theta)$  with respect to  $\theta$ , is simply  $\widehat{G}(\mathbf{w}^*, \lambda^*)$  with no additional optimizations.

We simulated from a linear regression model with  $n = 500$ ,  $p = 50$ , and  $\sigma_0^2 = 1$ . The true regression coefficient is set to be  $\{1, -2, 1, 0, \dots, 0\}$ , and each covariate vector  $X_i$  is



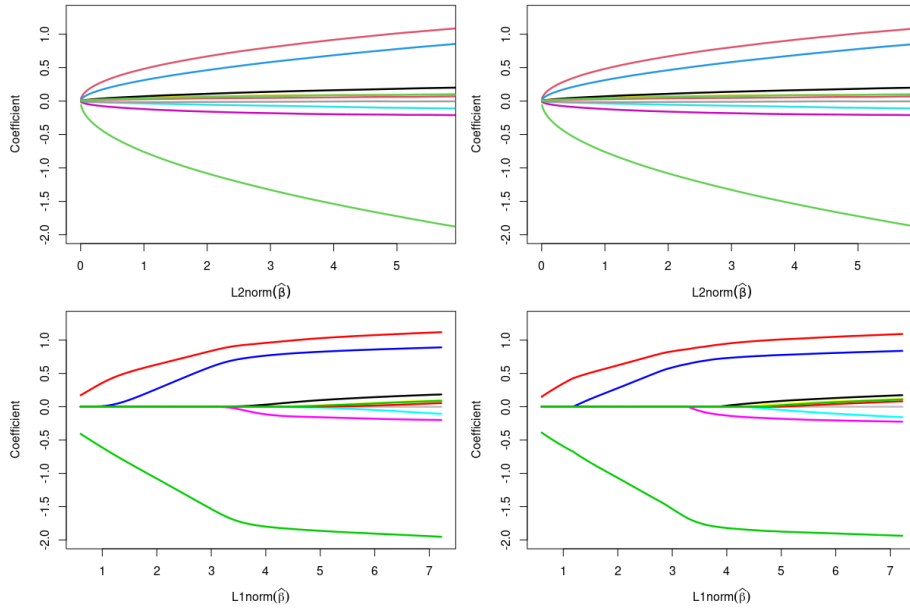


Figure 7: Solution paths of ridge (top row) and LASSO (bottom row) regressions obtained by the GMS (left column) and by LARS (right column).

independently generated from a  $N(0, \Sigma)$  with  $\Sigma_{kl} = 1$  for  $k = l$  and  $\Sigma_{kl} = 1/2$  for  $k \neq l$ . Figure 7 shows solution-path plots that depict the relations between the tuning parameter choices and the corresponding estimated ridge and LASSO estimators. The  $x$ -axis indicates the  $l_2$  norm of the ridge regression or  $l_1$  norm of the LASSO estimators based on a series of  $\lambda$ 's, and the  $y$ -axis, the value of the estimated coefficient. After the generator is trained by minimizing (7), ridge (top left) and LASSO (bottom left) coefficient values are just  $\hat{G}(\mathbb{1}, \lambda)$ , which generates the curves in Figure 7 by letting  $\lambda$  vary from 0.0006 to 0.6. The resulting solution-paths of the GMS ridge and LASSO procedures show that the proposed method approximates the standard ones obtained by LARS (Efron et al., 2004) very accurately.

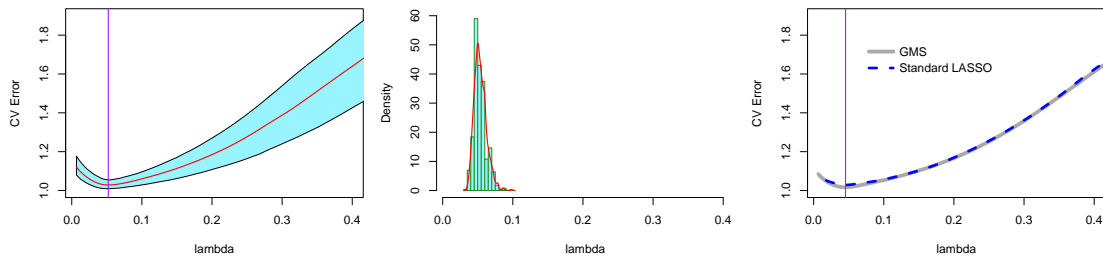


Figure 8: The 95% confidence band of CV error evaluated from the GMS bootstrap with random weights, and the red solid line indicates the mean curve (left); The GMS bootstrapped distribution of CV-error minimizers with respect to  $\lambda$  (middle); CV errors based on the standard LASSO and the GMS with a fixed weight of one (right). The purple vertical line indicates the value of  $\lambda$  that minimizes the CV error;  $\lambda = 0.052$  (left) and  $\lambda = 0.045$  (right).

We further investigate how GMS-bootstrap helps to quantify uncertainty in choosing  $\lambda$ . Figure 8 illustrates some benefits of the bootstrapped CV procedure for the LASSO example. The left panel shows a 95% confidence band for the CV errors across  $\lambda$ . As Efron and Tibshirani (1997) noted, the bootstrapped CV improves the performance of prediction error estimation. However, due to heavy computational burden in the standard bootstrap algorithm, applications of the bootstrapped CV have been greatly hindered. This example shows that the GMS can help overcome this computational difficulty. The center panel depicts the bootstrap distribution of the minimizer  $\lambda$  of the CV errors (the red line is the estimated density function). If the CV error curve is of main interest, one can easily generate it by the GMS using binary weights (corresponding to the chosen and left-out folds) as the input. As shown in the right panel of Figure 8, the CV error curve obtained by the standard CV computation is nearly identical to that given by the GMS.

### 4.3 Quantile regression

Quantile regression models, which assume that a certain quantile of the response variable linearly depends on the covariates, have been commonly used for robust regression analysis (Yu et al., 2003; Yu and Moyeed, 2001; Koenker, 2004). More precisely, for a given  $\eta \in (0, 1)$ , the conditional  $\eta$ -th quantile of the response given  $X_i$  is modeled by  $Q_Y(\eta; X_i) = X_i^T \theta$ . As a result, bootstrap samples of an estimate of  $\theta$  can be obtained by setting the loss function in (1) as

$$\ell(\theta; y_i, X_i) = \rho_\eta(y_i - X_i^T \theta), \quad (8)$$

where  $\rho_\eta(u) = (\eta - I(u < 0))u$ . The inference for the regression coefficients in this setting is more challenging than that for parametric regression models because the sampling distribution of the coefficient estimates often relies on the regression error density function, which needs to be estimated and is a challenging task by itself in high-dimensional settings (Koenker, 1994). In routine applications of quantile regression analyses, bootstrap procedures are popular to use for approximating the sampling distribution of the estimates (Feng et al., 2011; Hahn, 1995; Kocherginsky et al., 2005), which can be computationally very demanding. Furthermore, when a practitioner is interested in investigating multiple quantile levels, it is also necessary to repeat the bootstrap procedure multiple times, each at a different quantile level. Such a computational burden is prohibitive when the data size is large.

By using  $\ell(G(\mathbf{w}, \eta); y_i, X_i) = \rho_\eta(y_i - X_i^T G(\mathbf{w}, \eta))$  in (3), we apply the GMS to overcome the computational challenges for the inference of quantile regression models. The resulting loss of the GMS is

$$\hat{G} = \underset{G}{\operatorname{argmin}} \mathbb{E}_{\mathbf{w}, \eta} \left[ \sum_i^n w_i \rho_\eta(y_i - X_i^T G(\mathbf{w}, \eta)) \right], \quad (9)$$

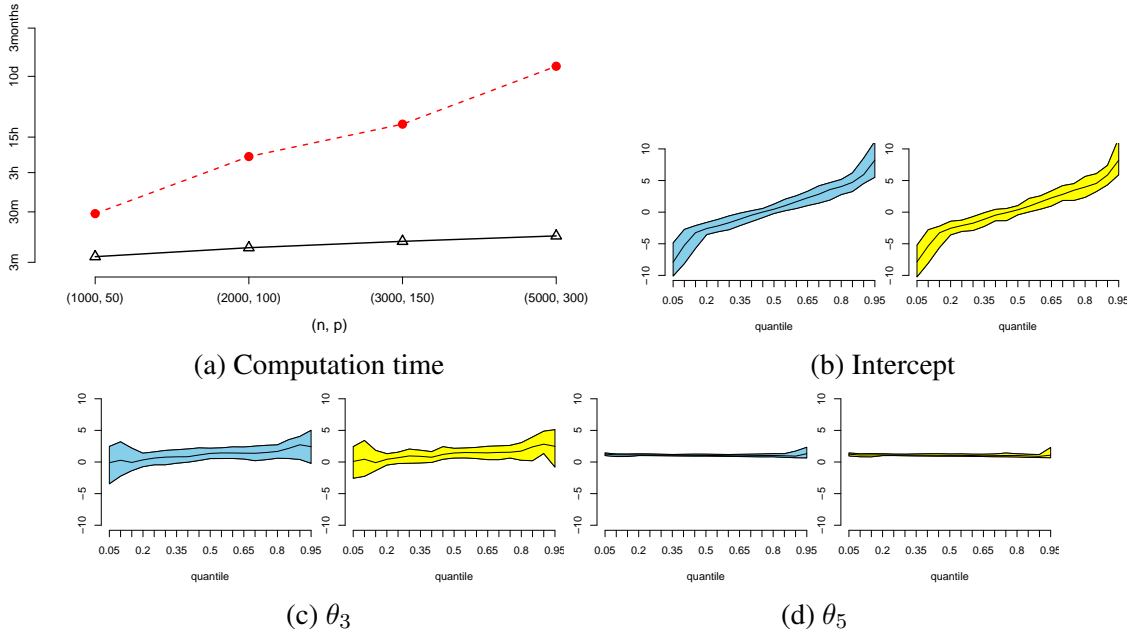


Figure 9: (a): The red dashed line and the black solid line indicate computation times for the standard bootstrap and the GMS version, respectively, in generating 5,000 bootstrap estimators; (b)–(d): Comparisons between 90% confidence bands from the GMS (blue) and the classical bootstrap (yellow) across quantile levels from 5% to 95%.

where  $\mathbb{E}_{\mathbf{w}, \eta}$  is the expectation operator on  $\mathbf{w}$  and  $\eta$ , assuming that  $\eta$  follows some distribution  $\mathbb{P}_\eta$  whose support is  $(0,1)$  and independent with  $\mathbf{w}$ . A default choice is that adding random noises to the candidate set of quantile levels, and  $\mathbf{w}$  follows the probability law in (6).

To demonstrate the effectiveness of this procedure, we test the method on a simulation example considered in Feng et al. (2011). The data set is generated from the model

$$y_i = X_i^\top \theta_0 + 3^{-1/2} [2 + \{1 + (x_{1i} - 8)^2 + x_{2i}\} / 10] \epsilon_i, \quad i = 1, \dots, n,$$

where  $X_i = (x_{i1}, \dots, x_{ip})^\top$ ,  $n = 500$ ,  $p = 5$ ,  $\theta_0 = (1, 1, 1, 1, 1)^\top$ , and  $\epsilon_i \sim t_3$ . We let  $x_{2i}$  be equal to 1 for  $i \leq 400$  and 0 for  $i > 400$ , and generate the other covariates independently from the standard log-normal distribution. Figure 9 (b)–(d) compare the 90% confidence bands of several coefficients generated by the GMS with those obtained by the standard bootstrap over quantiles varying from 0.05 and 0.95, showing that the approaches result in nearly identical bands.

To investigate computational efficiency of the GMS for quantile regression, we increase the sample size and the number of predictors in the above simulation model to  $(n, p) = (1000, 50)$ ,  $(2000, 100)$ ,  $(3000, 150)$ , and  $(5000, 300)$ , respectively, and consider quantile levels varying from 0.05 to 0.95 with a skip of 0.05 (total 19 quantile levels). We set the first five coefficients of  $\theta_0$  to be one and the others be zero. Our target is to obtain 5,000 bootstrap samples under each setting. Due to heavy computational burden

of the standard bootstrap procedure, we compute only five bootstrap evaluations and the reported computing time is approximated by multiplying 1,000 to the original time for the five evaluations. We use `quantreg` R package for the standard bootstrap of the quantile regression model. Figure 9 (a) depicts the time required for each procedure. While the GMS can be trained in less than 10 minutes for moderately large data size ( $n = 5000, p = 300$ ), the standard bootstrap procedure requires more than 30 minutes for even the smallest data set ( $n = 1000, p = 50$ ) and about 3 months for the case of ( $n = 5000, p = 300$ ) to compute 5,000 bootstrap estimators.

## 5 Bootstrapped Nonparametric MLE for Hierarchical Models

### 5.1 A variant of the GMS for NPMLE

Consider the following hierarchical mixture model:

$$y_i | \theta_i \sim \mathbb{F}_{\theta_i}, \quad \theta_i \stackrel{i.i.d.}{\sim} \pi, \quad \text{for } i = 1, \dots, n, \quad (10)$$

where  $\mathbb{F}_{\theta}$  is from a known distribution family characterized by parameter  $\theta \in \mathbb{R}^p$ , and  $\mathbf{Y} = \{y_1, \dots, y_n\}$  are the only observables. Kiefer and Wolfowitz (1956) proposed the *Nonparametric Maximum Likelihood Estimator* (NPMLE) for the mixture distribution  $\pi$  as

$$\hat{\pi} = \operatorname{argmax}_{\pi \in \Pi} \sum_{i=1}^n \log[\mathbb{E}_{\pi}\{f(y_i | \theta)\}], \quad (11)$$

where  $\Pi$  denotes the family of all possible distributions and  $f(y|\theta)$  is density or probability function of distribution  $\mathbb{F}_{\theta}$ . It is well-known that, under mild regularity conditions,  $\hat{\pi}$  exists and is unique, and even when the true mixture distribution is continuous, the optimal solution  $\hat{\pi}$  is a discrete measure supported on at most  $n$  points (Lindsay, 1995).

There exist several algorithms to solve (11), such as the EM algorithm (Laird, 1978; Jiang and Zhang, 2009; Dicker and Zhao, 2014) and convex optimization (Koenker and Mizera, 2014; Koenker and Gu, 2017). Alternatively, we can reformulate the nonparametric estimation problem of  $\pi$  in a generative framework. That is, we try to construct a NN-based “generator function”  $T$  so that  $T(\mathbf{z}) \sim \pi$ , where  $\mathbf{z} \in \mathbb{R}^q$  follows a known distribution such as Gaussian or uniform. Thus, the optimization problem (11) is turned into the following problem:

$$\hat{T} = \operatorname{argmax}_{T \in \mathcal{T}} \sum_{i=1}^n \log[\mathbb{E}_{\mathbf{z}}\{f(y_i | T(\mathbf{z}))\}], \quad (12)$$

where  $\mathbf{z} \in \mathbb{R}^q$  follows a known distribution such as  $\text{Unif}(0,1)$  when  $q = 1$ . This generative process was considered in Qiu and Wang (2021) by using the *Variational Auto-Encoder* (Kingma and Welling, 2013) accompanied by a bias-correction via a Langevin algorithm (Roberts and Tweedie, 1996; Dalalyan, 2017). However, both the standard NPMLE and this generative procedure result in discrete (or approximately discrete) mixture distributions, which is undesirable when the true mixture distribution is continuous as in many applications.

Bootstrapping is potentially one way to address the discreteness of NPMLE as the mean bootstrapped mixture distribution can be viewed as an approximation of the posterior mean Newton and Raftery (1994) and is much smoother than NPMLE. However, the standard bootstrap requires one to solve

$$\hat{\pi}^{*(b)} = \underset{\pi \in \Pi}{\operatorname{argmax}} \sum_{i=1}^n w_i^{(b)} \log[\mathbb{E}_{\pi}\{f(y_i | \theta)\}], \text{ where } \mathbf{w}^{(b)} \stackrel{\text{iid}}{\sim} \mathbb{P}_{\mathbf{w}}, \text{ for } b = 1, \dots, B,$$

which is quite time consuming. The GMS framework can be used to overcome the computational difficulty and obtain a continuous estimate of  $\pi$  simultaneously. With the integrative loss formulation, we obtain the *Generative Bootstrap NPMLE* (GB-NPMLE) as:

$$\hat{G} = \underset{G \in \mathcal{G}}{\operatorname{argmax}} \mathbb{E}_{\mathbf{w}} \left[ \sum_{i=1}^n w_i \log[\mathbb{E}_{\mathbf{z}}\{f(y_i | G(\mathbf{w}, \mathbf{z}))\}] \right]. \quad (13)$$

After training the generator function, we can easily generate samples from the bootstrapped mixture distribution of the NPMLE. For  $b = 1, \dots, B$ , we first sample  $\mathbf{w}^{(b)}$  and  $\mathbf{z}^{(b)}$  and evaluate  $\tilde{\theta}^{(b)} = \hat{G}(\mathbf{w}^{(b)}, \mathbf{z}^{(b)})$ . Table 2 shows that the results from GB-NPMLE and the standard bootstrap are nearly identical.

To improve the computational efficiency, we may use a subgroup bootstrap introduced in Section 3.1. The optimization of (13) can be simply implemented by modifying Algorithm 2 (see the appendix for details), and we approximate  $\log\{\mathbb{E}_{\mathbf{z}}\{f(y_i | G(\mathbf{w}, \mathbf{z}))\}\}$  by  $\log[\sum_{m=1}^M f(y_i | G(\mathbf{w}, \mathbf{z}^{(m)}))/M]$ , where the latent auxiliary variables  $\mathbf{z}^{(m)}$  are independently generated from  $\text{Unif}(0, 1)$  for  $m = 1, \dots, M$ . Even though using this Monte Carlo step for the stochastic optimization makes intuitive sense, this approximation poses a bias in approximating the gradient for the SGD due to the logarithm mapping shattering the linearity (Lian et al., 2017). However, we find that this bias is practically negligible, and we shall empirically examine the significance of the bias for the optimization in Section C.2 in the appendix.

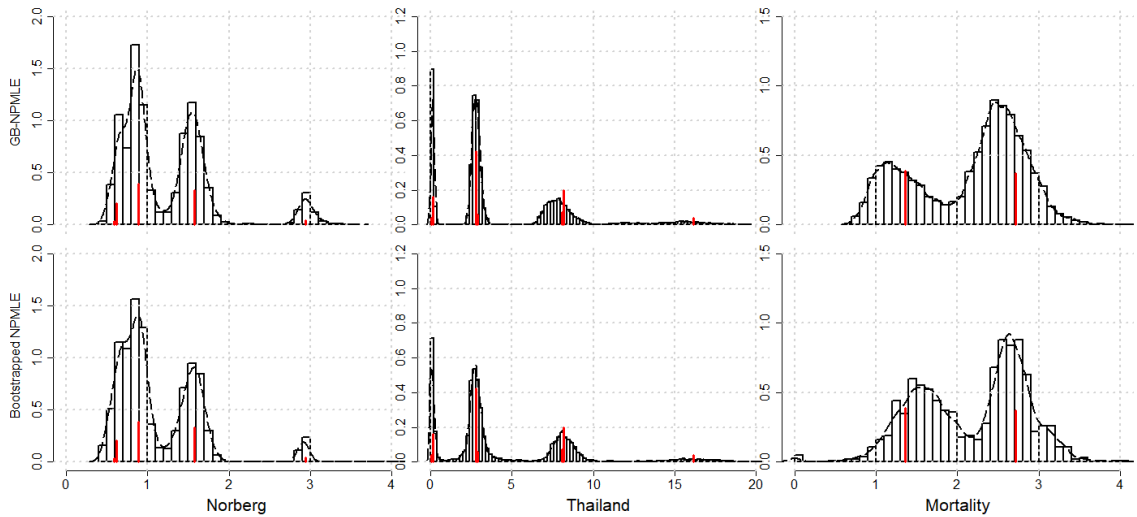


Figure 10: The estimated bootstrap NPMLE distributions for the GB-NPMLE (top) and the standard bootstrap (bottom); the black solid dash lines show the density of bootstrap distributions; the red vertical lines depict the discrete NPMLE solution.

## 5.2 A Poisson mixture example

The following Poisson mixture model has been frequently employed in analyzing counts data:

$$y_i \mid \theta_i \sim \text{Poisson}(\theta_i) \text{ and } \theta_i \sim \pi, \quad (14)$$

where  $\pi$  is a mixing distribution. We analyze three data sets studied in Böhning (1999): the *Norberg*, the *Thailand* and the *Mortality* data sets. The Norberg data set comprises 1,125 group life insurance statistics collected between 1982 and 1985 from a Norwegian insurance company (Norberg, 1989). The number of fatalities  $y_i$  and risk exposures are recorded to estimate the mixture distribution of the mean number of deaths. The Thailand data set consists of 602 pre-school children's health condition in Thailand from 1982 to 1985 (Böhning, 1999). The data set was collected in a cohort study, where the frequency of illness spells  $y_i$  were recorded for each child in a two-week period. The Mortality data set contains the number of deaths for women aged greater than or equal to 80 from the daily report of *Times* newspaper between 1910 and 1912. Using a single Poisson model for these data sets yields a poor fit due to over-dispersion and individual random effects. In contrast, the Poisson mixture distribution provides a more flexible prediction and identification of latent clustering effects.

Figure 10 compares the bootstrapped mixture distributions produced by the GB-NPMLE with those obtained by the standard bootstrap procedure with the convex optimization method for solving the NPMLE (Koenker and Mizera, 2014). The mixture distributions obtained by the two methods are nearly identical for aforementioned three data sets. Note that, for all the three examples, the NPMLE of  $\pi$  is discrete supported by very few points

Dataset	$n$	GB-NPMLE			Bootstrapped NPMLE		
		Width	Likelihood	Time (sec)	Width	Likelihood	Time (sec)
Norberg	72	2.33	20.35	126.1	2.39	20.83	732.8
Thailand	602	14.27	156.26	140.9	14.38	156.21	3439.3
Mortality	1096	2.29	199.30	153.3	2.25	199.31	5279.2

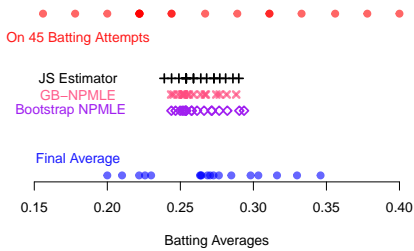
Table 2: Results for the Poisson mixture data sets: The width of 95% confidence region (“Width”) is evaluated by average of 20 replications. The logarithm of the out-of-sample predictive likelihood (“Likelihood”) of two procedures is evaluated by 10-fold cross validation with the same partition index.

(< 5) in the parameter space. In Table 2, due to the multimodal nature reflected in mixture components, we construct 95% confidence regions by means of *Highest Density Regions* (HDR) that represent the shortest interval, or the set of intervals, covering 95% probability of the mixture distribution. The overall widths of these regions (“Width”) are comparable between the two procedures. We also examine out-of-sample predictive performance  $\mathbb{E}_\theta[-\log f(\mathbf{Y}_{\text{new}}; \theta) \mid \mathbf{Y}_{\text{obs}}]$  under bootstrapping, which is reported as “Likelihood” in Table 2. More specifically, the out-of-sample “Likelihood” is evaluated by a 10-fold CV, such that  $\frac{1}{K} \sum_{k=1}^K \sum_{i \in I_k} -\log \left[ \frac{1}{B} \sum_{b=1}^B f(y_i; \hat{\theta}_b^{(-k)}) \right]$  where fold  $K = 10$ , number of bootstrap samples  $B = 500$  and  $\hat{\theta}_b^{(-k)} \sim \hat{\pi}_{(-k)}^*$ , where  $\hat{\pi}_{(-k)}^*$  is the bootstrap mixture distribution evaluated excluding the  $k$ -th fold. We note that the GB-NPMLE solutions are nearly identical to the corresponding standard bootstrap solutions, and the GB-NPMLE is much more computationally scalable. The computation time for the standard bootstrapped NPMLE increases nearly linearly in sample size, but remains nearly unchanged for the GB-NPMLE.

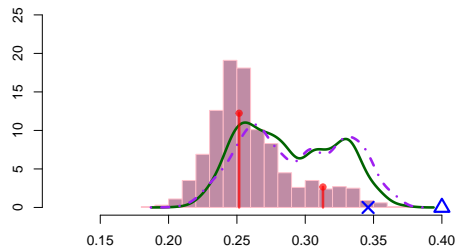
### 5.3 From bootstrapped NPMLE to empirical Bayes

The mixture model is naturally connected and mathematically equivalent to the empirical Bayes setup, if our interest is in evaluating an optimal prior distribution  $\theta_i$  in model (10), which can be empirically estimated. A classical nonparametric Bayes analysis starts by assuming a Dirichlet process prior on  $\pi$ . But the Dirichlet process also has some undesirable restrictions such as being almost surely discrete and being inconsistent in some cases (Diaconis and Freedman, 1986). Due to its connection with the Bayesian bootstrap (Newton and Raftery, 1994; Liu, 1996), the bootstrapped NPMLE appears to be a very good approximation without explicitly resorting to a formal prior on  $\pi$ . Note that the Bayesian bootstrap weight distribution  $\mathbf{w} \sim n \times \text{Dirichlet}(n, \mathbb{1}_n)$  corresponds to the posterior distribution under the Dirichlet process prior with the prior mass of the Dirichlet process converging to zero (Liu, 1996).

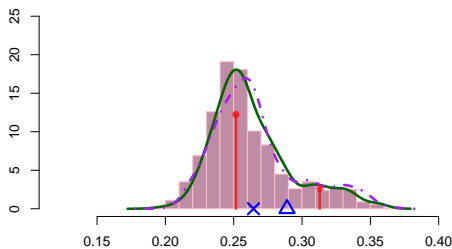
While numerous NPMLE procedures have been developed for empirical Bayes estimations (Dicker and Zhao, 2016; Jiang and Zhang, 2010; Gu and Koenker, 2017; Efron, 2019; Ignatiadis and Wager, 2021), bootstrap extensions have received little attention, perhaps due to their computational intensity. In the GMS framework, however, once the



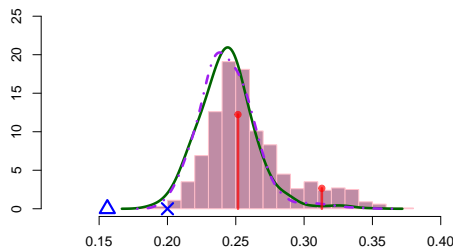
(a) Posterior means.



(b) Posterior distribution for “Clemente”.



(c) Posterior distribution for “Kessinger”.



(d) Posterior distribution for “Alvis”.

Figure 11: The baseball data set. (a) the posterior mean for each player; (b)–(d) the individual posterior distribution of the batting average  $\theta_i$  for several players. The histograms indicate the estimated bootstrapped NPMLE distribution  $\tilde{\pi}^*$  via the GB-NPMLE, while the green solid lines and the purple dash-dotted lines represent the individual posterior densities assessed by the GB-NPMLE and the conventional bootstrapped NPMLE, respectively. The blue crosses and the triangles indicate the final batting averages and the ones on 45 attempts, respectively. The red vertical peaks depict the standard NPMLE solutions computed by REBayes R package.

generator  $G$  is obtained, the evaluation of bootstrapped mixtures takes less than a second. For a future data point  $y'$ , the posterior predictive density  $p(y' | \mathbf{y})$  can be approximated by the mixture  $\frac{1}{N} [f(y' | \theta^{(1)}) + \dots + f(y' | \theta^{(N)})]$ , where  $\theta^{(k)} = G(\mathbf{w}^{(k)}, \mathbf{z}^{(k)})$  with  $(\mathbf{w}^{(k)}, \mathbf{z}^{(k)}) \sim \mathbb{P}_{\mathbf{w}} \times \mathbb{P}_{\mathbf{z}}$  for  $k = 1, \dots, N$ . Here we take  $\mathbb{P}_{\mathbf{w}} = n\text{Dir}(n; \mathbb{1}_n)$  and  $\mathbb{P}_{\mathbf{z}}$  be uniform on the  $q$ -dimensional unit cube (the dimension of  $\mathbf{w}$  can be reduced by the subgrouping method in Section 3.1) and  $q$  should be larger than the dimension of  $\theta$ .

**The baseball data.** We examine the baseball data set in Efron and Morris (1975), which contains the batting averages of 18 players during the 1970 *Major League Baseball* season. Efron and Morris (1975) analyzed the data by the empirical Bayes method and compared a few different shrinkage estimators including the *James-Stein* (JS) shrinkage estimator (James and Stein, 1961). The batting averages of the 18 players for the first 45 at-bats (attempts),  $y_i$  for  $i = 1, \dots, 18$ , as well as the final batting averages of these players at the end of the season, were recorded. Efron and Morris first transformed the data to  $x_i = f_{45}(y_i) = \sqrt{45}\arcsin(2y_i - 1)$  to stabilize the variance of the binomial distribution, where  $\mu_i = f_{45}(\theta_i)$ . Then, they assume  $\mu_i \sim N(\mu, \tau^2)$  and proceed with the empirical Bayes method. For the GB-NPMLE, the dimension of the latent random variable  $\mathbf{z}$  should be at least matched with the target dimension of the parameter  $p$ , and to ease the optimization of the generator function, we set a larger dimension  $q = 10$ .



Even though this is a landmark paper popularizing the empirical Bayes method, the Gaussianity severely constrains the shape of the unknown distribution  $\pi$ , and may miss important features of the mixture distribution. Rather than assuming a parametric form for  $\pi$ , researchers have considered a Bayesian nonparametric approach by imposing a Dirichlet process prior on  $\pi$  (Liu, 1996). However, the Dirichlet process is also quite restrictive as mentioned earlier. We here apply the more flexible GB-MLE to this problem.

Figure 11 (a) compares the posterior means of the JS estimator and the empirical Bayes estimators (means) by the GB-NPMLE and the standard bootstrapped NPMLE, respectively, demonstrating that all the three empirical Bayes methods agree with each other well. However, the posterior estimate of the mixing distribution  $\hat{\pi}$  (the shaded histogram in Figure 11 (b)–(d)) and the full NPMLE posterior density of each  $\theta_i$  (the overlaying curves in each subfigure) tell a lot more stories. It is obvious that the Gaussianity constraint is inappropriate for this example. The mixing distribution  $\hat{\pi}$  has two modes at 0.252 and 0.313 respectively, and is strongly right-skewed. As a result, the best batter among the 18 players, “Clemente”, has a near-symmetric bimodal posterior distribution, making its posterior mean estimate misleading. In contrast, the posterior distribution of the worst batter “Alvis” is nearly Gaussian. These results cannot be revealed by using the standard Gaussian hyper-prior.

## 6 Structures of Generator Function and Computational Strategies

### 6.1 Multilayer perceptron

*Neural Networks* (NN) have been shown effective for approximating functions with complicated structures. Recently, researchers have experimented with various novel ways of using neural networks, such as constructing generators of as complicated patterns as real-life images and creating generative adversarial networks for approximating high-dimensional distributions in a computationally feasible way (Ledig et al., 2017; Wang et al., 2018; Karras et al., 2018; Goodfellow et al., 2014; Arjovsky et al., 2017). The simplest NN structure is a class of *Multi-Layer Perceptrons* (MLP) constructed by composing activated linear transformations. For  $k = 1, \dots, K$ , let  $g_k$  denote the feed-forward mapping represented by  $N^{(k)}$  hidden nodes, where  $g_k : \mathbb{R}^{N^{(k)}} \mapsto \mathbb{R}^{N^{(k+1)}}$  is defined as

$$g_k(\mathbf{X}) = \sigma(\mathbf{U}^{(k)}\mathbf{X} + \mathbf{b}^{(k)}) \in \mathbb{R}^{N^{(k+1)}},$$

where  $\mathbf{X} \in \mathbb{R}^{N^{(k)}}$  is the input variable of  $g_k$ . Also, this function is characterized by a “weight” parameter and a “bias” parameter: the  $N^{(k+1)} \times N^{(k)}$  weight matrix  $\mathbf{U}^{(k)}$  and the  $N^{(k+1)}$ -dimensional bias vector  $\mathbf{b}^{(k)} = \{b_1^{(k)}, \dots, b_{N^{(k)}}^{(k)}\}$ , and the  $N^{(k+1)}$ -dimensional bias vector  $\mathbf{d}^{(k)}$ . Also,  $\sigma: \mathbb{R} \mapsto \mathbb{R}$  is called an *activation function*, and it operates element-

wise when the input is a vector or a matrix. A  $K$ -layered MLP function  $g : \mathbb{R}^{N^{(1)}} \mapsto \mathbb{R}^D$  can be defined by a composition of these functions as

$$g(\mathbf{X}) = L \circ g_K \circ \cdots \circ g_1(\mathbf{X}), \quad (15)$$

where  $L : \mathbb{R}^{N^{(K)}} \mapsto \mathbb{R}^D$  is a linear function that maps the final hidden layer  $g_K \circ \cdots \circ g_1(\mathbf{X})$  to the  $D$ -dimensional output space of  $g$ . Commonly used activation functions include the sigmoid (logistic) function, the hyperbolic tangent function, the *Rectified Linear Unit* (ReLU; Nair and Hinton (2010)), the *Exponential Linear Unit* (ELU; Clevert et al. (2015)), *Gaussian Error Linear Unit* (GELU; Hendrycks and Gimpel (2016)), and so on. For our generator, we use the ReLU function,  $\sigma(t) = \max\{t, 0\}$ , as a default. We here employ neural networks to construct the generator function  $G$  in (3) in a novel way as characterized by the integrative loss (3) and the weight multiplicative MLP explained below.

## 6.2 Weight multiplicative MLP

Despite its generalizability and practicability, we observe that the simple MLP converges slowly for our GMS and GBS applications (as shown by the example that will be discussed soon). We modify the simple MLP motivated by a Taylor approximation of the first derivative of the weighted loss function. Let us consider a weighted M-estimation loss  $\sum_{i=1}^n w_i \ell(\theta; y_i)$  and its optimizer  $\hat{\theta}_{\mathbf{w}}$  in (1) for a case of  $p = 1$  (ignoring  $\eta$  and  $\lambda$  for simplicity). Under mild conditions, we assume that  $\sum_{i=1}^n w_i \ell'(\hat{\theta}_{\mathbf{w}}; y_i) = 0$ , where  $\ell'$  is the first order derivative of  $\ell$ . Then, by using a Taylor approximation of  $\ell'$  at a local region of some arbitrary  $f(\mathbf{w})$ , we obtain that

$$0 = \sum_{i=1}^n w_i \ell'(\hat{\theta}_{\mathbf{w}}; y_i) \approx \sum_{i=1}^n w_i \ell'(f(\mathbf{w}); y_i) + \sum_{i=1}^n w_i \ell''(f(\mathbf{w}); y_i) (\hat{\theta}_{\mathbf{w}} - f(\mathbf{w})),$$

where  $\ell''$  are the second order derivatives of  $\ell$ . Thus, the approximated generator function follows that

$$\hat{\theta}_{\mathbf{w}} \approx f(\mathbf{w}) - \sum_{i=1}^n \frac{w_i \ell'(f(\mathbf{w}); y_i)}{\sum_{j=1}^n w_j \ell''(f(\mathbf{w}); y_j)} \triangleq f(\mathbf{w}) + \sum_{i=1}^n w_i h_i(\mathbf{w}), \quad (16)$$

Motivated by this approximation (16), we propose a new NN structure called the *Weight Multiplicative MLP* (WM-MLP) as a sum of a simple MLP and a weight multiplicative network:

$$G(\mathbf{w}, \lambda, \eta) = \underbrace{L_1 \circ B_K(\mathbf{w}, \lambda, \eta)}_{\substack{\text{Simple MLP:} \\ f(\mathbf{w})}} + \underbrace{L_2 \circ (\{g \circ B_K(\mathbf{w}, \lambda, \eta)\} \odot \mathbf{w})}_{\substack{\text{Weight multiplicative network:} \\ \sum_{i=1}^n w_i h_i(\mathbf{w}, \lambda, \eta)}}, \quad (17)$$

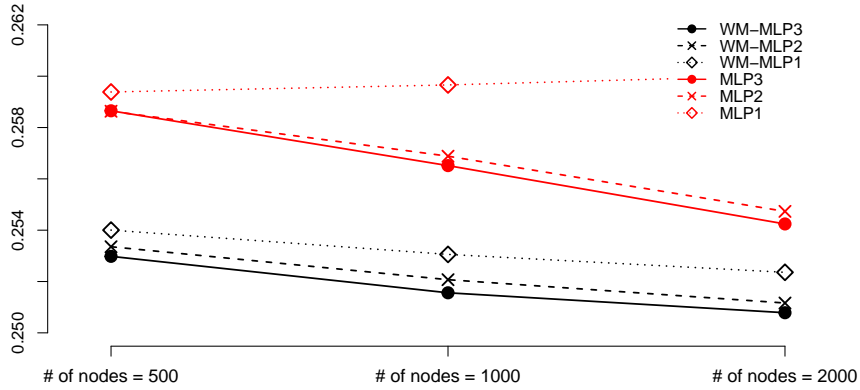


Figure 12: A loss comparison for the simple MLP and the WM-MLP with various numbers of hidden layers and nodes. The numbers noted after "MLP" indicate the number of layers  $K$ .

where “ $\odot$ ” indicates an element-wise multiplication operator;  $L_1 : \mathbb{R}^H \mapsto \mathbb{R}^p$  and  $L_2 : \mathbb{R}^n \mapsto \mathbb{R}^p$  are linear functions for some large enough positive integer  $H$ ;  $B_K : \mathbb{R}^{n+1+1} \mapsto \mathbb{R}^H$  and  $g : \mathbb{R}^H \mapsto \mathbb{R}^n$  are simple MLPs with  $K$  hidden layers and one hidden layer, respectively. When  $n$  is excessively large, we can use the subgrouping procedure in Section 3.1 to reduce the dimension of  $\mathbf{w}$  and the network size.

To demonstrate the improvement, we compare the performances of WM-MLP and the simple MLP, with various sizes of hidden nodes (500, 1000, 2000) and layers ( $K = 1, 2, 3$ ), for a logistic regression example. The true  $\theta$ 's in the simulations are equi-spaced between -0.5 and 0.5 with  $p = 100$  and  $n = 1000$ . We train the generator  $G$  from ten random initializations and report the average loss values after 30,000 iterative updates for each MLP structure. The results are summarized in Figure 12, demonstrating that for all network sizes, the proposed WM-MLP outperforms the simple MLP uniformly. In comparison to a large-sized MLP with three hidden layers and 2000 neurons, even a small-scale WM-MLP with a single hidden layer and 500 neurons achieves a lower loss, whereas the simple MLP with one hidden layer performs much poorly. In all considered examples, we used the WM-MLP with three hidden layers as a default, and observed that the resulting generator function based on the WM-MLP performed satisfactorily.

### 6.3 Computational strategy in optimization

It is straightforward to optimize the GMS integrative loss (3) because the expectation can be approximated by a few Monte Carlo samples at each iteration. We simply use a variant of the popular SGD algorithms such as *Adam* (Kingma and Ba, 2014), *AdaGrad* (Duchi et al., 2011), *RMSProp* (Tieleman et al., 2012), etc, to iteratively update the neural net parameters until the algorithm has converged. In Algorithm 2, a detailed algorithm for the GMS is demonstrated. As in (4), this algorithm samples  $M$  values of  $\mathbf{w}$ 's and  $\lambda$ 's to approximate the expectation and updates the NN parameters via SGD. It is not uncommon nowadays for a data set to be extremely large, to the point that the full data size surpasses

---

**Algorithm 2** A general algorithm to train the GMS.
 

---

- Set  $\mathbb{P}_{\alpha, \lambda, \eta}$ ,  $S$  (subgroup size),  $M$  (Monte Carlo sample size), and  $T$  (total iterations).
  - Randomly split the full data into  $S$  subgroups, resulting in an index function  $h(\cdot)$  in (6).
  - Initialize the neural net parameter  $\phi^{(0)}$ .
  - Set  $t = 0$ .
  - while** the stop condition is not satisfied or  $t < T$  **do**
    - Independently sample  $M$  values of  $\alpha$ 's,  $\lambda$ 's, and  $\eta$ 's from  $\mathbb{P}_{\alpha, \lambda, \eta}$ .
    - Consider 
$$L = \frac{1}{M} \sum_{m=1}^M \sum_{i=1}^n \alpha_{h(i)}^{(m)} l(G_{\phi^{(t)}}(\alpha^{(m)}, \lambda^{(m)}, \eta^{(m)}); y_i) / n + \lambda^{(m)} u(G_{\phi^{(t)}}(\alpha^{(m)}, \lambda^{(m)}, \eta^{(m)})),$$
 where  $\alpha^{(m)}$  is the  $m$ -th sample of  $M$   $\alpha$ 's.
    - Update  $\phi^{(t+1)}$  by using the gradient of  $L$  via a SGD step.
    - Let  $t = t + 1$ .
- 
- end while**
- 

the memory capacity of the computer in use. Data subsampling would be advantageous in this setting for training the GMS, which partially updates the weights corresponding to the subsampled data in the same spirit as stochastic optimization.

Under mild regularity conditions, the convergence of SGD based on a general Monte Carlo approximation is guaranteed. According to a theory established by Allen-Zhu et al. (2019), if the NN's inputs are non-degenerate and the network is over-parameterized, i.e., the number of neurons is at a polynomial rate of  $n$  and  $l$ , where  $l$  is the number of hidden layers, simple SGDs and GDs, such as Algorithm 2, achieve the *global optima* in polynomial time of  $n$  and  $l$ .

**Technical details of the optimization.** In all our examples, We use the MLP with three hidden layers and 1,000 hidden neurons in each layer. In `PyTorch`, algorithm Adam is used with a learning rate of 0.0003 and a decay rate of  $t^{-0.3}$  by default. We use full samples in the SGD optimization without mini-batches because the data sizes of the examples we considered are manageable. However, when the data size is massive, minibatch subsampling would be necessary.

**Choosing distributions for  $\mathbf{w}$ ,  $\lambda$ , and  $\eta$ .** For bootstrap procedures, the distribution of bootstrap weights  $\mathbf{w}$  (or  $\alpha$ ) can be easily chosen depending on the practitioner's interest. One may set

$$\mathbf{w} \sim \text{Multinomial}(n, \mathbb{1}_n/n) \quad \text{or} \quad \mathbf{w} \sim n \times \text{Dirichlet}(n, \mathbb{1}_n)$$

for nonparametric and Bayesian bootstrap, respectively. When  $n$  is excessively large, the dimension of  $\mathbf{w}$  can be reduced by the subgroup bootstrapping method in Section 3.1. As a general rule, when  $n > 500$ , we recommend considering subgrouping. While theoretical evidence suggests that  $S \asymp n^{1/2}$  is optimal, empirically setting  $S$  to a few hundreds performs well in all situations shown in this paper. By default,  $S = 100$  was used. For CV procedures, either bootstrapped or standard, the weight distribution proposed in Algorithm 1 can be used. Choosing the training distributions for  $\lambda$  and  $\eta$  is more arbitrary

because usually we have no reference distributions for  $\lambda$  and  $\eta$ . We may first set candidate sets for  $\lambda$  and  $\eta$  in advance (which can be large in size) and then add some random noises to form mixture distributions. For example, we can generate  $\lambda = \exp\{\log \lambda' + \epsilon\}$ , where  $\lambda'$  is randomly selected from the candidate set and  $\epsilon \sim N(0, \delta)$  with  $\delta = 0.2^2$  as default. For the quantile regression example in Section 4.2, we generate  $\eta = \eta' + N(0, 0.03^2)$  with  $\eta'$  randomly selected from a pre-determined candidate set, and then truncated to be in  $(0.001, 0.999)$ .

## 7 Conclusion

We propose the GMS as a general computational framework to accelerate repeated calculations for (penalized) weighted M-estimations. The GMS was shown effective for a variety of statistical inference procedures, including bootstrap methods, cross-validations, and nonparametric empirical Bayes. We apply the GMS to a variety of models, including LASSO, quantile regression, logistic regression, and NPMLE. The GMS performs well in all of the situations we investigated, and the weighted M-estimators generated by the GMS are sufficiently accurate and comparable to the much more computationally expensive traditional solutions for all inference purposes. By lowering the computational barrier associated with repetitious data-splitting or data-sampling processes such as bootstrapped CVs, iterated bootstrap, and bootstrapped empirical Bayes, the GMS opens up a new perspective on modern statistics. To date, these approaches have been less noticed and rarely practiced by the statistical community not because they are less valuable, but because their computation cost is prohibitively high. We expect that the GMS will prove to be an effective tool for augmenting the power of statistical models in the era of big data.

## References

- Allen-Zhu, Z., Li, Y., and Song, Z. (2019). A convergence theory for deep learning via over-parameterization. In *International Conference on Machine Learning*, pages 242–252. PMLR.
- Arjovsky, M., Chintala, S., and Bottou, L. (2017). Wasserstein generative adversarial networks. In *International Conference on Machine Learning*, pages 214–223.
- Barbe, P. and Bertail, P. (2012). *The weighted bootstrap*, volume 98. Springer Science & Business Media.
- Böhning, D. (1999). *Computer-assisted analysis of mixtures and applications: meta-analysis, disease mapping and others*, volume 81. CRC press.
- Bühlmann, P. (2002). Bootstraps for time series. *Statistical science*, pages 52–72.
- Chatterjee, S., Bose, A., et al. (2005). Generalized bootstrap for estimating equations. *The Annals of Statistics*, 33(1):414–436.
- Cheng, G. and Huang, J. Z. (2010). Bootstrap consistency for general semiparametric m-estimation. *The Annals of Statistics*, 38(5):2884–2915.
- Clevert, D.-A., Unterthiner, T., and Hochreiter, S. (2015). Fast and accurate deep network learning by exponential linear units (elus). *arXiv preprint arXiv:1511.07289*.
- Cybenko, G. (1989). Approximation by superpositions of a sigmoidal function. *Mathematics of control, signals and systems*, 2(4):303–314.
- Dalalyan, A. (2017). Further and stronger analogy between sampling and optimization: Langevin monte carlo and gradient descent. In *Conference on Learning Theory*, pages 678–689. PMLR.
- Diaconis, P. and Freedman, D. (1986). On inconsistent bayes estimates of location. *The Annals of Statistics*, pages 68–87.
- Diciccio, T. and Efron, B. (1992). More accurate confidence intervals in exponential families. *Biometrika*, 79(2):231–245.
- Dicker, L. H. and Zhao, S. D. (2014). Nonparametric empirical bayes and maximum likelihood estimation for high-dimensional data analysis. *arXiv preprint arXiv:1407.2635*.
- Dicker, L. H. and Zhao, S. D. (2016). High-dimensional classification via nonparametric empirical bayes and maximum likelihood inference. *Biometrika*, 103(1):21–34.
- Duchi, J., Hazan, E., and Singer, Y. (2011). Adaptive subgradient methods for online learning and stochastic optimization. *Journal of machine learning research*, 12(7).

- Efron, B. (1979). Bootstrap methods: Another look at the jackknife. *The Annals of Statistics*, 7(1):1–26.
- Efron, B. (1987). Better bootstrap confidence intervals. *Journal of the American statistical Association*, 82(397):171–185.
- Efron, B. (2019). Bayes, oracle bayes and empirical bayes. *Statistical science*, 34(2):177–201.
- Efron, B., Hastie, T., Johnstone, I., and Tibshirani, R. (2004). Least angle regression. *The Annals of statistics*, 32(2):407–499.
- Efron, B. and Morris, C. (1975). Data analysis using stein’s estimator and its generalizations. *Journal of the American Statistical Association*, 70(350):311–319.
- Efron, B. and Tibshirani, R. (1997). Improvements on cross-validation: the 632+ bootstrap method. *Journal of the American Statistical Association*, 92(438):548–560.
- Efron, B. and Tibshirani, R. J. (1994). *An introduction to the bootstrap*. CRC press.
- Feng, X., He, X., and Hu, J. (2011). Wild bootstrap for quantile regression. *Biometrika*, 98(4):995–999.
- Geer, S. A., van de Geer, S., and Williams, D. (2000). *Empirical Processes in M-estimation*, volume 6. Cambridge university press.
- Giné, E. and Zinn, J. (1990). Bootstrapping general empirical measures. *The Annals of Probability*, pages 851–869.
- Goodfellow, I., Pouget-Abadie, J., Mirza, M., Xu, B., Warde-Farley, D., Ozair, S., Courville, A., and Bengio, Y. (2014). Generative adversarial nets. In *Advances in neural information processing systems*, pages 2672–2680.
- Gu, J. and Koenker, R. (2017). Empirical bayesball remixed: Empirical bayes methods for longitudinal data. *Journal of Applied Econometrics*, 32(3):575–599.
- Hahn, J. (1995). Bootstrapping quantile regression estimators. *Econometric Theory*, 11(1):105–121.
- Hall, P. (1986). On the bootstrap and confidence intervals. *The Annals of Statistics*, pages 1431–1452.
- Hall, P. (1988). Theoretical comparison of bootstrap confidence intervals. *The Annals of Statistics*, pages 927–953.
- Hall, P. (1992). On bootstrap confidence intervals in nonparametric regression. *The Annals of Statistics*, pages 695–711.

- Hall, P. (2013). *The bootstrap and Edgeworth expansion*. Springer Science & Business Media.
- Hall, P. and Martin, M. A. (1988). On bootstrap resampling and iteration. *Biometrika*, 75(4):661–671.
- Härdle, W., Horowitz, J., and Kreiss, J.-P. (2003). Bootstrap methods for time series. *International Statistical Review*, 71(2):435–459.
- Hendrycks, D. and Gimpel, K. (2016). Gaussian error linear units (gelus). *arXiv preprint arXiv:1606.08415*.
- Huber, P. J. (1992). Robust estimation of a location parameter. In *Breakthroughs in statistics*, pages 492–518. Springer.
- Ignatiadis, N. and Wager, S. (2021). Confidence intervals for nonparametric empirical bayes analysis. *Journal of the American Statistical Association*. To appear.
- Isola, P., Zhu, J.-Y., Zhou, T., and Efros, A. A. (2017). Image-to-image translation with conditional adversarial networks. In *Proceedings of the IEEE conference on computer vision and pattern recognition*, pages 1125–1134.
- James, W. and Stein, C. (1961). Estimation with quadratic loss. 1(1961):361–379.
- Jiang, W. and Zhang, C.-H. (2009). General maximum likelihood empirical bayes estimation of normal means. *Annals of Statistics*, 37(4):1647–1684.
- Jiang, W. and Zhang, C.-H. (2010). Empirical bayes in-season prediction of baseball batting averages. In *Borrowing Strength: Theory Powering Applications—A Festschrift for Lawrence D. Brown*, pages 263–273. Institute of Mathematical Statistics.
- Karras, T., Aila, T., Laine, S., and Lehtinen, J. (2018). Progressive growing of gans for improved quality, stability, and variation. In *International Conference on Learning Representations*.
- Kiefer, J. and Wolfowitz, J. (1956). Consistency of the maximum likelihood estimator in the presence of infinitely many incidental parameters. *The Annals of Mathematical Statistics*, pages 887–906.
- Kingma, D. P. and Ba, J. (2014). Adam: A method for stochastic optimization. *arXiv preprint arXiv:1412.6980*.
- Kingma, D. P. and Welling, M. (2013). Auto-encoding variational bayes. *arXiv preprint arXiv:1312.6114*.



- Kleiner, A., Talwalkar, A., Sarkar, P., and Jordan, M. I. (2014). A scalable bootstrap for massive data. *Journal of the Royal Statistical Society: Series B (Statistical Methodology)*, 76(4):795–816.
- Kocherginsky, M., He, X., and Mu, Y. (2005). Practical confidence intervals for regression quantiles. *Journal of Computational and Graphical Statistics*, 14(1):41–55.
- Koenker, R. (1994). Confidence intervals for regression quantiles. In *Asymptotic statistics*, pages 349–359. Springer.
- Koenker, R. (2004). Quantile regression for longitudinal data. *Journal of Multivariate Analysis*, 91(1):74–89.
- Koenker, R. and Gu, J. (2017). Rebayes: an r package for empirical bayes mixture methods. *Journal of Statistical Software*, 82(1):1–26.
- Koenker, R. and Mizera, I. (2014). Convex optimization, shape constraints, compound decisions, and empirical bayes rules. *Journal of the American Statistical Association*, 109(506):674–685.
- Kosorok, M. R. (2008). M-estimators. *Introduction to Empirical Processes and Semiparametric Inference*, pages 263–282.
- Lahiri, S. N. (1999). Theoretical comparisons of block bootstrap methods. *Annals of Statistics*, pages 386–404.
- Laird, N. (1978). Nonparametric maximum likelihood estimation of a mixing distribution. *Journal of the American Statistical Association*, 73(364):805–811.
- Ledig, C., Theis, L., Huszár, F., Caballero, J., Cunningham, A., Acosta, A., Aitken, A., Tejani, A., Totz, J., Wang, Z., et al. (2017). Photo-realistic single image super-resolution using a generative adversarial network. In *Proceedings of the IEEE conference on computer vision and pattern recognition*, pages 4681–4690.
- Lee, S. M. and Young, G. A. (1995). Asymptotic iterated bootstrap confidence intervals. *The Annals of Statistics*, pages 1301–1330.
- Lee, S. M. and Young, G. A. (1999). The effect of monte carlo approximation on coverage error of double-bootstrap confidence intervals. *Journal of the Royal Statistical Society: Series B (Statistical Methodology)*, 61(2):353–366.
- Lian, X., Wang, M., and Liu, J. (2017). Finite-sum Composition Optimization via Variance Reduced Gradient Descent. In Singh, A. and Zhu, J., editors, *Proceedings of the 20th International Conference on Artificial Intelligence and Statistics*, volume 54 of *Proceedings of Machine Learning Research*, pages 1159–1167. PMLR.

- Lindsay, B. G. (1995). Mixture models: theory, geometry and applications. In *NSF-CBMS regional conference series in probability and statistics*, pages i–163. JSTOR.
- Liu, J. S. (1996). Nonparametric hierarchical bayes via sequential imputations. *The Annals of Statistics*, pages 911–930.
- Lu, Z., Pu, H., Wang, F., Hu, Z., and Wang, L. (2017). The expressive power of neural networks: A view from the width. In *Proceedings of the 31st International Conference on Neural Information Processing Systems*, pages 6232–6240.
- Martin, M. A. (1992). On the double bootstrap. In *Computing science and statistics*, pages 73–78. Springer.
- McCarthy, D., Zhang, K., Brown, L. D., Berk, R., Buja, A., George, E. I., and Zhao, L. (2018). Calibrated percentile double bootstrap for robust linear regression inference. *Statistica Sinica*, 28(4):2565–2589.
- Nair, V. and Hinton, G. E. (2010). Rectified linear units improve restricted boltzmann machines. In *Proceedings of the 27th International Conference on International Conference on Machine Learning*, pages 807–814.
- Newton, M. A. and Raftery, A. E. (1994). Approximate Bayesian inference with the weighted likelihood bootstrap. *Journal of the Royal Statistical Society: Series B (Methodological)*, 56(1):3–26.
- Norberg, R. (1989). Experience rating in group life insurance. *Scandinavian Actuarial Journal*, 1989(4):194–224.
- Præstgaard, J. and Wellner, J. A. (1993). Exchangeably weighted bootstraps of the general empirical process. *The Annals of Probability*, pages 2053–2086.
- Qiu, Y. and Wang, X. (2021). Almond: Adaptive latent modeling and optimization via neural networks and langevin diffusion. *Journal of the American Statistical Association*, 116(535):1224–1236.
- Roberts, G. O. and Tweedie, R. L. (1996). Exponential convergence of langevin distributions and their discrete approximations. *Bernoulli*, pages 341–363.
- Rubin, D. B. (1981). The Bayesian bootstrap. *The Annals of Statistics*, 9(1):130434.
- Rumelhart, D. E., Hinton, G. E., and Williams, R. J. (1986). Learning representations by back-propagating errors. *nature*, 323(6088):533–536.
- Tibshirani, R. (1996). Regression shrinkage and selection via the lasso. *J. R. Statist. Soc. B*, pages 267–288.

- Tieleman, T., Hinton, G., et al. (2012). Lecture 6.5-rmsprop: Divide the gradient by a running average of its recent magnitude. *COURSERA: Neural networks for machine learning*, 4(2):26–31.
- Wang, T.-C., Liu, M.-Y., Zhu, J.-Y., Tao, A., Kautz, J., and Catanzaro, B. (2018). High-resolution image synthesis and semantic manipulation with conditional gans. In *Proceedings of the IEEE conference on computer vision and pattern recognition*, pages 8798–8807.
- Xu, L., Gotwalt, C., Hong, Y., King, C. B., and Meeker, W. Q. (2020). Applications of the fractional-random-weight bootstrap. *The American Statistician*, pages 1–21.
- Yu, K., Lu, Z., and Stander, J. (2003). Quantile regression: applications and current research areas. *Journal of the Royal Statistical Society: Series D (The Statistician)*, 52(3):331–350.
- Yu, K. and Moyeed, R. A. (2001). Bayesian quantile regression. *Statistics & Probability Letters*, 54(4):437–447.

# Supplementary Material of “Generative Multiple-purpose Sampler for Scalable Weighted M-estimation”

## A Theoretical Justification of Subgroup Bootstrap

While subgrouping was shown empirically to approximate the target bootstrap distribution well, its theoretical consistency is not immediately apparent. Here we employ the theoretical tools described in Cheng and Huang (2010) to examine theoretical aspects of subgrouping bootstrap procedures for the general M-estimation. Let  $Y_1, Y_2, \dots$  be a sequence of iid random variables (with their observed values  $y_1, y_2, \dots$ ) from the probability distribution  $\mathbb{P}_0$  with the true parameter  $\theta_0$ , and the resulting expectation is denoted by  $\mathbb{E}_0$ . The probability distribution of  $\mathbf{w}$  and its expectation are denoted by  $\mathbb{P}_{\mathbf{w}}$  and  $\mathbb{E}_{\mathbf{w}}$ , respectively. The empirical measure of the observations and the expectation with respect to it are denoted by  $\hat{P}_n$  and  $\hat{\mathbb{E}}_n$ , respectively. We also define a weighted bootstrap empirical measure  $\hat{\mathbb{P}}_{\mathbf{w},n} = \sum_{i=1}^n w_i \delta_{y_i} / n$ , where  $\delta_t$  is a point measure at  $t$ , and the expectation with respect to it is denoted by  $\hat{\mathbb{E}}_{\mathbf{w},n}$ . We let  $\ell'$  and  $\ell''$  denote the first and second order derivatives of  $\ell(\theta; Y)$  with respect to  $\theta$ , respectively. The original M-estimator, which corresponds to the solution of (1) with  $\mathbf{w} = \mathbf{1}$ , is denoted by  $\hat{\theta}$ . The big “ $O_{\mathbb{P}_0}$ ” and small “ $o_{\mathbb{P}_0}$ ” are based on probability distribution  $\mathbb{P}_0$ . We then consider some regularity conditions below:

- (A1) There exists  $\epsilon > 0$  such that  $\mathbb{E}_0[\ell'(\theta) - \ell'(\theta_0)] = \mathbb{E}_0[\ell''(\theta_0)(\theta - \theta_0)] + O(\|\theta - \theta_0\|^2)$ , if  $\|\theta - \theta_0\| < \epsilon$  for large enough  $n$ .
- (A2) Suppose that  $\mathbb{E}_0[\ell'(\theta_0)] = 0$ ,  $\hat{\mathbb{E}}_n[\ell'(\hat{\theta})] = o_{\mathbb{P}_0}(\sqrt{n})$ , and  $\hat{\mathbb{E}}_{\mathbf{w},n}[\ell'(\hat{\theta}_{\mathbf{w}})] = o_{\mathbb{P}_0}(\sqrt{n})$ . Also, assume that the optimizers  $\hat{\theta}$  and  $\hat{\theta}_{\mathbf{w}}$  are unique over  $\mathcal{W}$ .
- (A3) There exists  $\delta > 0$  such that  $\hat{\mathbb{E}}_n[\ell'(\theta) - \ell'(\theta_0)] - \mathbb{E}_0[\ell'(\theta) - \ell'(\theta_0)] = O_{\mathbb{P}_0}(\sqrt{n}\|\theta - \theta_0\|)$ , if  $\|\theta - \theta_0\| < \delta$ .
- (A4) The variance of  $\ell'(\theta_0)$  and  $\mathbb{E}_0[\ell''(\theta_0)]$  are both non-singular.

These or similar mild regularity conditions are often required for showing asymptotic consistency of M-estimators as in (Kosorok, 2008; Geer et al., 2000). Condition (A1) assures that the derivative of the loss is smooth enough to be linearly approximated around a local region at the true parameter. Condition (A2) assumes the uniqueness of the minimizers, and is general enough to deal with the case that the estimator and its bootstrap version are not exact minimizers, but “nearly-minimizing” the target losses. Condition (A3) is called the *stochastic equi-continuity* (Cheng and Huang, 2010) and guarantees that the discrepancy between the empirical and true derivatives of the loss around the true parameter is of order  $\sqrt{n}$ . Condition (A4) ensures that the considered estimator asymptotically attains a non-singular variance.

under the same regularity conditions described in Section 3.1. They considered the

following set of conditions on the weight distribution to guarantee the bootstrap consistency:

- W1. The distribution of the weight vector  $\mathbf{w} = \{w_1, \dots, w_n\}$  is exchangeable for all  $n = 1, \dots$ .
- W2.  $w_i \geq 0$  for all  $i$  and  $\sum_{i=1}^n w_i = n$ .
- W3. For some positive constant  $C < \infty$ ,  $\limsup_{n \rightarrow \infty} \|w_1\|_{2,1} \leq C$ , where  $\|w_1\|_{2,1} = \int_0^\infty \sqrt{P_{\mathbf{w}}(w_1 \geq u)} du$ .
- W4.  $\lim_{\lambda \rightarrow \infty} \limsup_{n \rightarrow \infty} \sup_{t \geq \lambda} t^2 P_{\mathbf{w}}(w_1 > t) = 0$ .
- W5.  $\sum_{i=1}^n (w_i - 1)^2 / n \xrightarrow{P} c^2$  with respect to  $\mathbb{P}_{\mathbf{w}}$  for some constant  $c > 0$ .

Under these conditions, Theorem 1 in Cheng and Huang (2010) for the bootstrap consistency states that:

**Theorem A.1.** (Cheng and Huang, 2010). Assume that (A1) – (A4) hold, and the subgroups are randomly assigned. Consider a random weight bootstrap with  $\mathbf{w} \sim \mathbb{P}_{\mathbf{w}}$  that satisfy W1–W5. Then, the resulting subgroup bootstrap is consistent; i.e.,

$$\sup_{x \in \mathbb{R}^p} \left| \mathbb{P}_{\mathbf{w}|D_n}(\sqrt{n}(\hat{\theta}_{\mathbf{w}} - \hat{\theta}) \leq x) - \mathbb{P}_0(\sqrt{n}(\hat{\theta} - \theta_0) \leq x) \right| \rightarrow 0,$$

in  $\mathbb{P}_0$ -probability as  $n$  tends to  $\infty$ .

The condition of W2 is also clearly true. Since the marginal distribution of  $w_1$  follows Beta(1,  $S - 1$ ), W3 and W4 are satisfied. For W5, because  $\mathbb{E}\{(w_1 - 1)^2\} = 1 - 2/(S + 1)$ , the subgroup weights satisfy W5.

Now it is sufficient to show that the exchangeability holds as in W1 to show the consistency of the bootstrap. However, the members of each subgroup is fixed in advance, which breaks the exchangeability condition among the bootstrap weights. Instead of using the exchangeability, we show that the subgroup bootstrap is consistent with a bootstrap procedure based on an exchangeable bootstrap weights, which guarantees the consistency of our subgroup bootstrap.

As an opponent of the proposed fixed subgrouped weight  $\mathbf{w}_S = \{w_{S,1}, \dots, w_{S,n}\}$  with deterministic subgroup indexes  $\{I_1, \dots, I_S\}$ , we first consider a fully randomized subgroup bootstrap weight  $\tilde{\mathbf{w}}_S = \{\tilde{w}_{S,1}, \dots, \tilde{w}_{S,1}\}$  that assumes the subgroups are also randomly assigned for every bootstrap evaluation. Like the subgroup weights, its weights are also generated from  $\{\tilde{\alpha}_{S,1}, \dots, \tilde{\alpha}_{S,S}\} \sim S \times \text{Dirichlet}(S, \mathbb{1}_S)$ . As a result, it is trivial that the distribution of  $\tilde{\mathbf{w}}_S$  is exchangeable, as well as satisfying W2–W5. Then, it follows

that for any bounded and continuous function  $f$ ,

$$\begin{aligned} \text{Var} \left( \frac{1}{\sqrt{n}} \sum_{i=1}^n (w_{S,i} - 1) f(y_i) \mid \mathbf{y} \right) &= \mathbb{E} \left( \left\{ \frac{1}{\sqrt{n}} \sum_{i=1}^n (w_{S,i} - \tilde{w}_{S,i} + \tilde{w}_{S,i} - 1) f(y_i) \right\}^2 \mid \mathbf{y} \right) \\ &= \mathbb{E} \left( \left\{ \frac{1}{\sqrt{n}} \sum_{i=1}^n (w_{S,i} - \tilde{w}_{S,i}) f(y_i) \right\}^2 \mid \mathbf{y} \right) \dots \dots \dots \quad (\text{A1}) \end{aligned}$$

$$+ 2\mathbb{E} \left( \left\{ \frac{1}{\sqrt{n}} \sum_{i=1}^n (w_{S,i} - \tilde{w}_{S,i}) f(y_i) \right\} \left\{ \frac{1}{\sqrt{n}} \sum_{i=1}^n (\tilde{w}_{S,i} - 1) f(y_i) \right\} \mid \mathbf{y} \right) \dots \dots \dots \quad (\text{A2})$$

$$+ \text{Var} \left( \frac{1}{\sqrt{n}} \sum_{i=1}^n (\tilde{w}_{S,i} - 1) f(y_i) \mid \mathbf{y} \right) \dots \dots \dots \quad (\text{A3}).$$

Because the fully randomized subgroup bootstrap is consistent, the corresponding variance part (A3) in the above equation should be non-zero. As a result, it is sufficient to show that the other term (A1) + (A2) converges to zero in probability with respect to the probability measure  $\mathbb{P}_{\mathbf{y}}$ .

After a simple arithmetic, it follows that

$$\begin{aligned} &(\text{A1}) + (\text{A2}) \\ &= \frac{1}{n} \mathbb{E} \left( \left\{ \sum_{i=1}^n w_{S,i} f(y_i) \right\}^2 - \left\{ \sum_{i=1}^n \tilde{w}_{S,i} f(y_i) \right\}^2 \mid \mathbf{y} \right) \\ &= \frac{1}{n} \mathbb{E} \left( \left\{ \sum_{s=1}^S \alpha_{S,s} \sum_{i \in I_s} f(y_i) \right\}^2 - \left\{ \sum_{s=1}^S \tilde{\alpha}_{S,s} \sum_{i \in \tilde{I}_s} f(y_i) \right\}^2 \mid \mathbf{y} \right). \end{aligned}$$

Because  $\text{Var}(\alpha_{S,1}) = \frac{S-1}{(S+1)}$  and  $\text{Cov}(\alpha_{S,1}, \alpha_{S,2}) = -\frac{1}{(S+1)}$ , the above equation follows that

$$\begin{aligned} &(\text{A1})+(\text{A2}) \\ &= \frac{S-1}{n(S+1)} \sum_{s=1}^S \left[ \left\{ \sum_{i \in I_s} f(y_i) \right\}^2 - \mathbb{E}_{\tilde{I}} \left( \left\{ \sum_{i \in \tilde{I}_s} f(y_i) \right\}^2 \mid \mathbf{y} \right) \right] \dots \dots \dots \quad (\text{B1}) \\ &+ \frac{1}{n(S+1)} \sum_{s \neq k} \left[ \left\{ \sum_{i \in I_s} f(y_i) \right\} \left\{ \sum_{i \in I_k} f(y_i) \right\} - \mathbb{E}_{\tilde{I}} \left( \left\{ \sum_{i \in \tilde{I}_s} f(y_i) \right\} \left\{ \sum_{i \in \tilde{I}_k} f(y_i) \right\} \mid \mathbf{y} \right) \right]. \end{aligned}$$

We show that the variance of (B1) converges to zero as  $n$  grows. Then, by using similar steps, we can show that the rest part converges to zero as well. Because  $\sum_{s=1}^S \sum_{i \in I_s} f(y_i)^2 =$

$\sum_{i=1}^n f(y_i)^2$  for any exclusive subgroups  $\{I_1, \dots, I_S\}$ , it follows that

$$\begin{aligned}
\text{Var}\{(\mathbf{B1})\} &= \text{Var} \left[ \frac{S-1}{n(S+1)} \sum_{s=1}^S \left\{ \sum_{\substack{i,l \in I_s \\ i \neq l}} f(y_i)f(y_l) - \mathbb{E}_{\tilde{I}} \left( \sum_{\substack{i,l \in \tilde{I}_s \\ i \neq l}} f(y_i)f(y_l) \mid \mathbf{y} \right) \right\} \right] \\
&\leq 2\text{Var} \left[ \frac{S-1}{n(S+1)} \sum_{s=1}^S \sum_{\substack{i,l \in I_s \\ i \neq l}} f(y_i)f(y_l) \right] \\
&= \frac{2(S-1)^2}{n^2(S+1)^2} \sum_{s=1}^S \text{Var} \left[ \sum_{\substack{i,l \in I_s \\ i \neq l}} f(y_i)f(y_l) \right] \\
&= \frac{2S(S-1)^2}{n^2(S+1)^2} \left[ 4(n/S)(n/S-1)\text{Var}\{f(y_1)f(y_2)\} \right. \\
&\quad \left. + 8(n/S)(n/S-1)(n/S-2)\text{Cov}\{f(y_1)f(y_2), f(y_1)f(y_3)\} \right]
\end{aligned}$$

Then, the variance term is  $O(S^{-1})$  and the covariance term is at a rate of  $O(n/S^2)$ . Therefore, the variance of (B1) converges to zero when  $S \succ n^{1/2}$ .  $\square$

## B Details of Double Bootstrap Procedures

We first introduce notation here. Let  $F_0$  and  $\widehat{F}_n$  denote the true distribution function and the empirical distribution of the observed data set, respectively. The bootstrapped version, which is resulted from random sampling the observations with replacement, of  $\widehat{F}_n$  is denoted by  $\widehat{F}_n^*$ . In the same sense, the distribution of double bootstrapped observations, which is a bootstrapped version of  $\widehat{F}_n^*$ , is denoted by  $\widehat{F}_n^{**}$ . We denote the single-bootstrap and double bootstrap estimators resulted from  $\widehat{F}_n^*$  and  $\widehat{F}_n^{**}$  by  $\hat{\theta}^*$  and  $\hat{\theta}^{**}$ , respectively. We let the expectation operators  $\mathbb{E}_0$  and  $\widehat{\mathbb{E}}_n$  be with respect to  $F_0$  and  $\widehat{F}_n$ , respectively.

It is well-known that percentile (or bootstrap-t) CI via a single bootstrap procedure is not calibrated well in a sense that the resulting bootstrapped coverage is not matched to the nominal coverage, and the CI based on these procedures are unnecessarily wide (Efron and Tibshirani, 1994). For a one-sided CI with 95% nominal coverage, the basic idea of these bootstrap is on the following approximation:

$$\mathbb{P}(T^* > t_\alpha^* \mid \widehat{F}_n) \approx \mathbb{P}_0(T > t_\alpha \mid F_0) = 1 - \alpha,$$

where *i*)  $T = \hat{\theta} - \theta_0$  for the percentile procedure; *ii*)  $T = (\hat{\theta} - \theta_0)/s$ , where  $s$  is the standard error (when unknown, we set  $s = 1$ ), for the studentized procedure, and  $t_\alpha$  is the  $\alpha$  quantile of the distribution of  $T$ . Also,  $T^*$  and  $t_\alpha^*$  are bootstrapped versions of  $T$  and  $t_\alpha$ , respectively. Despite their simple and bootstrap-like intuition, the problem is that the

bootstrapped probability  $\mathbb{P}(T^* > t_\alpha^* \mid \widehat{F}_n)$  can be significantly deviated from the target coverage  $1 - \alpha$  in finite samples.

To relieve this problem, Hall and Martin (1988) considered a double bootstrap to calibrate the coverage error for the percentile procedure. This correction searches for a valid quantile level  $\widehat{\alpha}$  in a way that the resulting bootstrap coverage probability approximates  $1 - \alpha$ ; i.e.,  $\mathbb{P}(T^* > t_{\widehat{\alpha}}^* \mid \widehat{F}_n) \approx 1 - \alpha$ . We can approximate such  $\widehat{\alpha}$  by using a double bootstrap, and a bootstrap version of  $\mathbb{P}(T^* > t_\alpha^* \mid \widehat{F}_n)$  can be evaluated via a double-bootstrapped probability  $\mathbb{P}(T^{**} > t_\alpha^{**} \mid \widehat{F}_n^*)$ , where  $T^{**}$  and  $t_\alpha^{**}$  are a double-bootstrapped counterpart of  $T^*$  and  $t_\alpha^*$ . The solution  $\widehat{\alpha}$  can be evaluated by a Monte Carlo approximation as the following steps:

1. Evaluate  $T_b^* = \widehat{\theta}_b^* - \widehat{\theta}$  and  $T_{bc}^{**} = \widehat{\theta}_{bc}^{**} - \widehat{\theta}_b^*$  for  $b = 1, \dots, B$  and  $c = 1, \dots, C$ .
2. Construct  $u_b^* = \frac{1}{C} \sum_{c=1}^C \mathbf{1}(T_{bc}^{**} > T_b^*)$  for  $b = 1, \dots, B$ .
3. Set  $\widehat{\alpha} = u_{(B(1-\alpha))}^*$ , where  $u_{(h)}^*$  is the  $h$ -th smallest ordered value of  $\{u_1^*, \dots, u_B^*\}$ .

Then, the calibrated CI can be constructed by  $(\infty, \widehat{\theta} + t_{\widehat{\alpha}}^*)$  for the percentile procedure.

The other approach of double bootstraps is to estimate the standard error of  $\widehat{\theta}_b^* - \widehat{\theta}$  for the studentized procedure (Hall, 1988). The explicit form of the bootstrap standard error  $\widehat{s}_b^*$  of  $\widehat{\theta}_b^*$  is frequently unknown, and the second level bootstrap of the  $b$ -th bootstrap data set can be used to evaluate the standard deviation of  $\widehat{\theta}_b^*$ ; i.e.,  $\widehat{s}_b^* \approx \sqrt{\sum_{c=1}^C (T_{bc}^{**} - \bar{T}_b^*)^2 / (C - 1)}$ , where  $\bar{T}_b^* = \sum_{c=1}^C T_{bc}^{**} / C$ . Then, the resulting one-sided CI with 95% level is  $(\infty, \widehat{\theta} + \tilde{t}_{95\%}^* \widehat{s})$ , where  $\tilde{t}_\beta^*$  is the  $\beta$ -quantile of  $\{(\widehat{\theta}_b^* - \widehat{\theta}) / \widehat{s}_b^*\}_{b=1, \dots, B}$ , and  $\widehat{s}$  is the estimated standard error of  $\widehat{\theta}$  from the single bootstrap distribution. By following a similar way, one can construct a two-sided confidence interval by changing lower and upper levels of quantile values.

## C Supplementary materials for GB-NPMLE

### C.1 GB-NPMLE two-stage algorithm

In order to capture the underlying mixture structure  $\pi$ , we generalize the output of generator  $G$  to be  $\mathbb{R}^{q \times p}$ . By setting  $q = 1$  is equivalent to GMS, while under  $q \geq 2$ , the resultant  $\theta_{1:q,j}$ , serves as bootstrap sample candidates which help recognize unknown mixture distribution  $\pi$ . Nonetheless, this modest characterization leads to correlation across bootstrap samples  $\theta_{1:q,j}$  where  $j \in \{1, \dots, p\}$ . To address correlation problem, we slightly alter Algorithm 2 and propose a *Two-stage GB-NPMLE* Algorithm 3.



**Algorithm 3 Stage I:** Fix  $\boldsymbol{\tau} = \{\tau_1, \dots, \tau_q\}$  where  $\tau_1 = \dots = \tau_q = 1/q$

$$\widehat{G} = \underset{G}{\operatorname{argmin}} \frac{1}{N} \sum_{k=1}^N \left[ \sum_{i=1}^n w_i^{(k)} \log \left( \frac{1}{M} \sum_{m=1}^M f[y_i | G(\mathbf{w}^{(k)}, \mathbf{z}^{(m)})_{|\Lambda}] d\Phi(\mathbf{z}) \right) \right], \quad (18)$$

where  $G(\mathbf{w}^{(k)}, \mathbf{z}^{(m)})_{|\Lambda}$  represents the output matrix of generator  $\theta_{q \times p}$  is sliced by index matrix  $\Lambda$ , resulting in  $\theta_{1 \times p}$ .

In Algorithm 3 Stage I, also known as  $G$  training stage, the key step lies in randomly generating an indexing matrix  $\Lambda_{q \times p}$  for generator output  $\theta_{q \times p}$ . The indexing matrix  $\Lambda_{q \times p}$  is generated in a way such that  $\Lambda = [\gamma_1, \dots, \gamma_p]$  and each vector  $\gamma_j \sim \text{Multinomial}(1, \boldsymbol{\tau} = \{\tau_1, \dots, \tau_q\})$  where  $j \in \{1, \dots, p\}$  with an equal and fixed mixture probability  $\boldsymbol{\tau} = \{1/q, \dots, 1/q\}$ . In other words, when training  $G$  in stage I, Algorithm 3 overcomes correlation issue by taking one  $\theta_p^*$  out of  $\theta_{1,p}, \dots, \theta_{q,p}$  for each  $p$  according to mixture probability  $\boldsymbol{\tau}$ .

**Algorithm 3 Stage II:** Fix the trained generator  $\widehat{G}$  and update  $\boldsymbol{\tau}$  via EM algorithm.

$$\tau_k^{(t+1)} = \frac{1}{n} \sum_{i=1}^n \frac{\tau_k^{(t)} \cdot \frac{1}{M} \sum_{m=1}^M [f(y_i | \widehat{G}(\mathbf{w}^{(m)}, \mathbf{z}^{(m)})_{|\Gamma_{q,i}})]}{\sum_{k=1}^q \tau_k^{(t)} \cdot \frac{1}{M} \sum_{m=1}^M [f(y_i | \widehat{G}(\mathbf{w}^{(m)}, \mathbf{z}^{(m)})_{|\Gamma_{q,i}})]}, \quad (19)$$

where  $\widehat{G}(\mathbf{w}^{(m)}, \mathbf{z}^{(m)})$  is a trained generator and  $\Gamma_{q,i}$  is set to be a  $q \times p$  indexing matrix with  $i$ th column being 1 and others being 0 such that  $[\mathbf{0}_{q \times 1}, \dots, \mathbf{1}_{q \times 1}, \dots, \mathbf{0}_{q \times 1}]$ .

After obtaining a well-trained generator  $\widehat{G}$  from Stage I, Algorithm 3 Stage II involves optimization of mixture probability  $\boldsymbol{\tau}$ . Realizing that  $\theta_{q \times p}$  is fixed when  $\widehat{G}$  is fixed, we implement EM algorithm as a golden choice for optimizing  $\boldsymbol{\tau}$ . The convergence of EM algorithm in this scenario is expected to be fairly fast in that bootstrap sample candidates is well-optimized and therefore mixture probability  $\boldsymbol{\tau}$  can be easily trained. A summary of *Two-stage GB-NPMLE* Algorithm is present next in Algorithm 3.

The proposed Algorithm 3 allows GMS (or GBS for bootstrap purpose here) to be more capable of capturing unknown mixture structure than directly implementing GMS Algorithm 2 under NPMLE case. To illustrate its fast-convergence, we take into account of a rather complicated Gaussian Mixture model(GMM) which is characterized by following designed structure,

---

**Algorithm 3** GB-NPMLE Two-stage Algorithm
 

---

- 1: *Initialize* the value of  $N$ ,  $M$ ,  $q$  and  $S$ .
- 2: *Initialize* the neural net (NN) parameter along with learning rate, hidden size and epoch value  $T$ .
- 3: **procedure:** Optimization Stage I
- 4:   **for**  $t$  in  $1, \dots, \text{Epoch } T$  **do**
- 5:     Generate  $\Lambda$ ,  $\mathbf{w}$  and  $\mathbf{z}$
- 6:     Evaluate loss (18) as  $Loss^{(t)} = \frac{1}{N} \sum_{k=1}^N \left[ \sum_{i=1}^n w_i^{(k)} \log\left(\frac{1}{M} \sum_{m=1}^M f[y_i \mid G(\mathbf{w}^{(k)}, \mathbf{z}^{(m)})_{|\Lambda}] d\Phi(\mathbf{z})\right) \right]$
- 7:     Minimizing Loss via SGD
- 8:   **end for**
- 9:   **Return**  $\hat{G}$
- 10: **end procedure**
- 11: **procedure:** Optimization Stage II
- 12:   *Initialize*  $tol = 0.001$ ,  $\tau^{new} = \{1/q, \dots, 1/q\}$  and  $\tau^{old} = \{0, \dots, 0\}$
- 13:   **while**  $\min(|\tau^{old} - \tau^{new}|) \geq tol$  **do**
- 14:      $\tau^{old} = \tau^{new}$
- 15:     Updating  $\tau^{new}$  by (19):  $\tau_k^{(t+1)} = \frac{1}{n} \sum_{i=1}^n \frac{\tau_k^{(t)} \cdot \frac{1}{M} \sum_{m=1}^M [f(y_i | \hat{G}(\mathbf{w}^{(m)}, \mathbf{z}^{(m)})_{|\Gamma_{\mathbf{q}, i}})]}{\sum_{k=1}^q \tau_k^{(t)} \cdot \frac{1}{M} \sum_{m=1}^M [f(y_i | \hat{G}(\mathbf{w}^{(m)}, \mathbf{z}^{(m)})_{|\Gamma_{\mathbf{q}, i}})]}$
- 16:   **end while**
- 17:   **Return**  $\hat{\tau}$
- 18: **end procedure**

---

$$y_i \mid \theta_i \sim \text{Normal}(\mu_i = \theta_i, \sigma = 0.5) \text{ and } \theta_i = \begin{cases} 2, & \text{w.p } 0.2 \\ 4, & \text{w.p } 0.3 \\ 6, & \text{w.p } 0.4 \\ 20, & \text{w.p } 0.1, \end{cases} \text{ for } i = 1, \dots, 10000 \quad (20)$$

In this simulation study, we set the total training epoch  $T$  to be 5,000 for both Algorithm 2 and Algorithm 3 in purpose of performance comparison. During the training stage, loss values in (21) of two algorithms are evaluated and recorded every ten seconds respectively. When evaluating loss (21), we choose  $(J, M)$  to be (100, 1000) for a better Monte Carlo approximation while avoiding potential *GPU* memory storage issue.

$$\begin{aligned} \text{Algorithm 1 loss} &= -\frac{1}{J} \sum_{j=1}^J \left[ \sum_{i=1}^n w_i^{(j)} \log \left( \frac{1}{M} \sum_{m=1}^M f(y_i \mid \hat{G}(\mathbf{w}^{(j)}, \mathbf{z}^{(m)})) d\Phi(\mathbf{z}) \right) \right] \\ \text{Algorithm 3 loss} &= -\frac{1}{J} \sum_{j=1}^J \left[ \sum_{i=1}^n w_i^{(j)} \log \left( \frac{1}{M} \sum_{m=1}^M f(y_i \mid \hat{G}(\mathbf{w}^{(j)}, \mathbf{z}^{(m)})_{|\hat{\Lambda}(\hat{\tau})}) d\Phi(\mathbf{z}) \right) \right] \end{aligned} \quad (21)$$

In Figure 13, we show how the loss values are optimized as time changes based on recorded loss of two algorithms. The smoothed trend of loss values is also depicted in Figure 13, which summarizes the simulation findings. It is evident that Algorithm 2 converges substantially more slowly than Algorithm 3. GMS Algorithm 2 takes approxi-

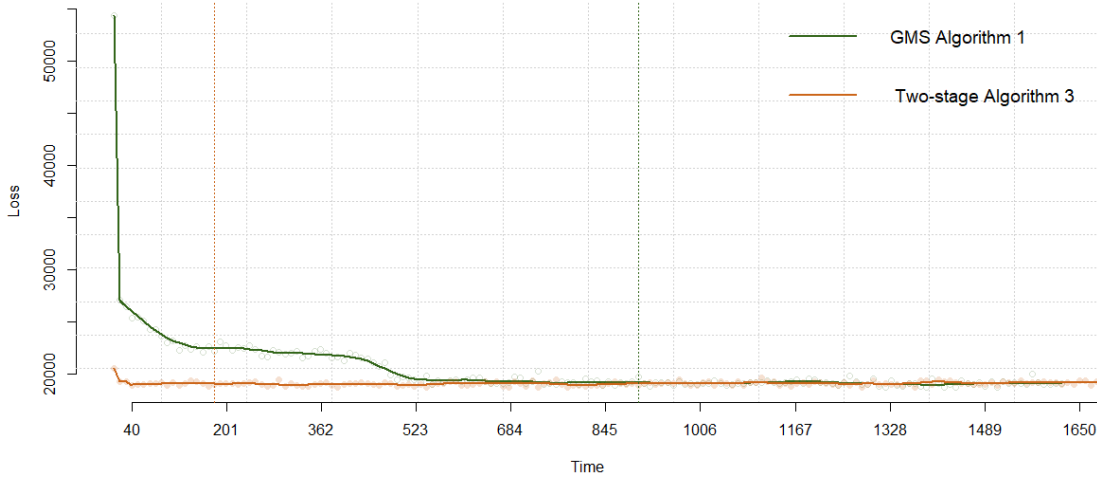


Figure 13: Green and orange dots represent loss values of two algorithms; the green and orange trend line is drawn by *lowess smoothing*; green dotted vertical line positions Algorithm 2 at time 900 and orange dotted vertical line positions Algorithm 3 at time 180.

mately 1,000 seconds (nearly 15 minutes) to stabilize the loss optimization to some level. While in contrast, Algorithm 3 exhibits faster convergence time, taking roughly 3 minutes to achieve nearly the same loss level as Algorithm 2 does.

## C.2 GB-NPMLE Robustness Analysis

Regarding the implementation of proposed GB-NPMLE, we need to initialize the value of hyperparameter  $(M, N, q)$  in 18. As indicated by strong law of large number, we ideally prefer a sufficient large value  $(M, N)$  for better Monte Carlo approximation. However, as  $(M, N)$  grows larger, the desired approximation is traded at the cost of increased computational burden. Therefore, we have to be cautious with  $(M, N)$  as well as  $q$  since the number of replications  $q$  is directly related to the inference of underlying mixture structure  $\pi$ . To investigate how sensitive the final optimization outcome is to different  $(M, N, q)$ , we perform a robustness analysis on GB-NPMLE Algorithm 3.

In our robustness simulation study, we consider a simple mixture linear regression model, such that  $y_i = x_i \cdot \theta_i + \epsilon_i$  where  $\epsilon_i$  follows i.i.d  $N(0, 0.1)$ . The true regression coefficient  $\theta_i$  is assumed to follow a designed two-component mixture distribution.

$$\theta_i = \begin{cases} -1, & \text{w.p } 0.5 \\ +1, & \text{w.p } 0.5 \end{cases} \quad (22)$$

One sample size of 10,000 dataset is randomly generated and GB-NPMLE Algorithm 3 is implemented accordingly. Each time one of the hyperparameters  $(M, N, q)$  is allowed to change across distinct values while the rest two remains constant at  $(100, 100)$ . To assess the impact of hyperparameters, we mainly focus on two factors that reflect the

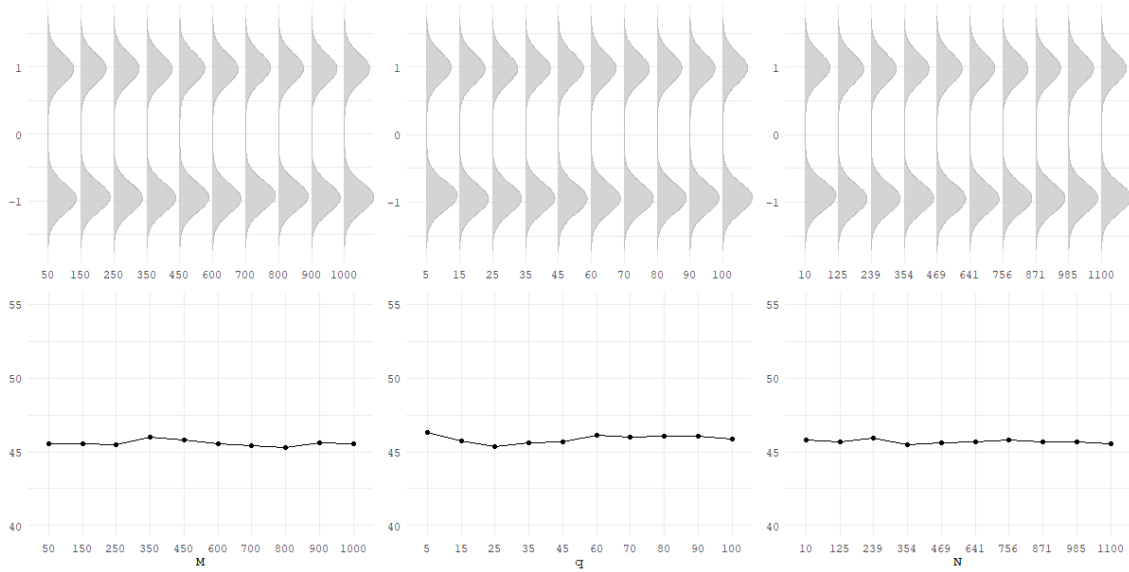


Figure 14: The histogram of bootstrap samples across different  $(M, N, q)$  (top); The estimated *loss* across across different  $(M, N, q)$  (bottom).

robustness of GB-NPMLE, which are the distribution of resulting bootstrap samples and loss value respectively. Figure 14 shows that the resulting NPMLE bootstrap distributions from GB-NPMLE Algorithm 3, are almost consistent and robust to  $(M, N, q)$ . Furthermore, the corresponding loss values also reveal that changing  $(M, N, q)$  has little impact on GB-NPMLE optimization. Therefore, in consideration of computational cost, we set  $(M, N, q)$  to be  $(100, 100, 100)$  as default for GB-NPMLE Algorithm 3.

### C.3 GB-NPMLE mixture model Analysis

In addition to Poisson mixture model (PMM) investigated in real data analysis Section 5.2, we consider the other three classic and commonly-used mixture models such as Gaussian Mixture model (GMM), Binomial Mixture model (BMM) and Gamma Mixture model (GaMM). In our designed study, these three mixture models can be represent as a discrete mixture format, such that  $y|\theta \sim p_1 \cdot f(y|\theta_1) + p_2 \cdot f(y|\theta_2)$  where  $(p_1, p_2)$  denotes the true mixture probability for  $(\theta_1, \theta_2)$ . Furthermore, as an illustration of smoothing effect of bootstrapping on discrete NPMLE solution, we revisit PMM model where unknown distribution  $\pi$  is instead assumed to follow Gamma distribution, a smooth density.

1. *Gaussian Mixture Model* (GMM):  $y | \theta \sim \text{Normal}(\mu = \theta, \sigma = 0.5)$  and  $\theta = \begin{cases} 0, & \text{w.p } 0.8 \\ 2, & \text{w.p } 0.2 \end{cases}$
2. *Gamma Mixture Model* (GaMM):  $y | \theta \sim \text{Gamma}(1, \theta)$  and  $\theta = \begin{cases} 1, & \text{w.p } 0.2 \\ 10, & \text{w.p } 0.8 \end{cases}$
3. *Binomial Mixture Model* (BMM):  $y | \theta \sim \text{Binomial}(n = 10, p = \theta)$  and  $\theta = \begin{cases} 0.2, & \text{w.p } 0.5 \\ 0.8, & \text{w.p } 0.5 \end{cases}$

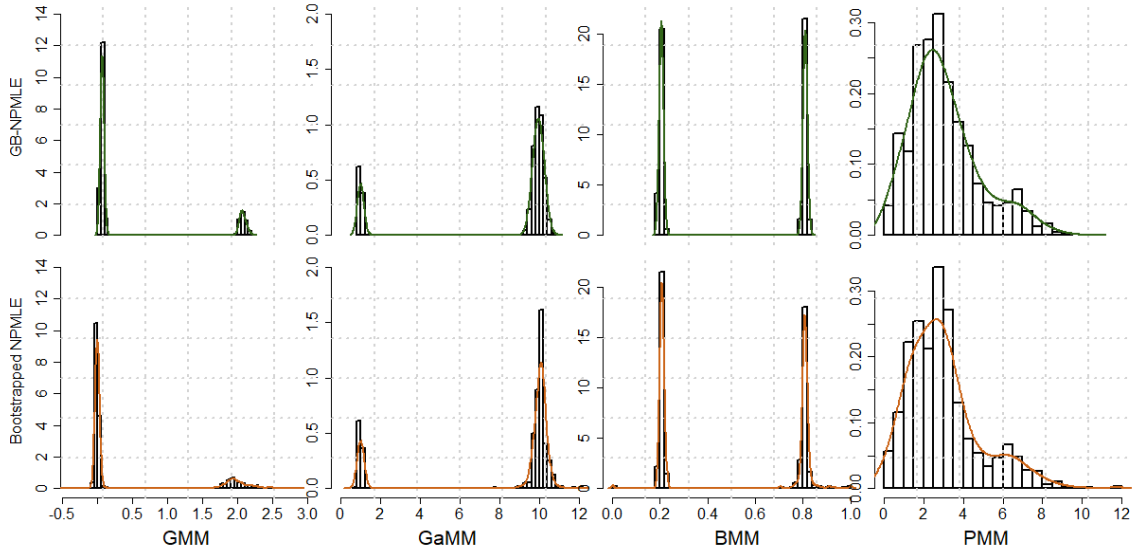


Figure 15: The green and orange solid line represents the smoothed density plot;

Model	GB-NPMLE ( $n = 100$ )				$n = 1,000$		$n = 10,000$		Bootstrapped NPMLE ( $n = 100$ )				$n = 1,000$		$n = 10,000$	
	Width	$\ell_1$ error	Cov	Time	Time	Time	Width	$\ell_1$ error	Cov	Time	Time	Time	Time	Time	Time	
GMM	0.586	0.064	0.95	140	161	423	0.625	0.049	0.95	425	4020	31620				
BMM	0.533	0.018	1	180	222	661	0.568	0.016	1	90	150	320				
GaMM	1.048	0.338	1	87	114	384	0.974	0.371	1	488	4400	44880				
PMM	4.178	0.958	0.97	140	189	326	4.151	0.973	0.99	1175	5040	49020				

Table 3: Averaged results based on 100 replications; HPD Cov (Cov) and HPD Width (Width) measures the coverage rate and width of 95% HPD interval;  $\ell_1$ error is defined such that  $\frac{1}{n} \sum_{i=1}^n \{|\theta_i - E(\theta_i | y_i)|\}_1$ .

#### 4. Poisson Mixture Model (PMM): $\mathbf{y} | \theta \sim \text{Poisson}(\theta)$ and $\theta \sim \text{Gamma}(3, 1)$

The detailed summary of these four mixture model settings is given above. We evaluate the performance of GB-NPMLE Algorithm 3 as well as standard bootstrap procedure on all four mixture cases.

As a result, Figure 15 depicts the resultant bootstrapping distribution based on 1,000 bootstrap samples respectively. The first three mixture setting (GMM, GaMM and BMM) are all discrete cases and we see that GB-NPMLE bootstrap distribution is almost identical to the standard NPMLE bootstrap distribution. Besides that, GB-NPMLE reveals approximately the same mixture probability  $(p_1, p_2)$  as that of standard bootstrap. Moreover in continuous PMM mixture setting, GB-NPMLE Algorithm 3 exhibits its capability of dealing with continuous mixture density  $\pi$ , remarkably close to standard bootstrap distribution.

In addition, table 3 presents different numerical comparison measures such as 95%HPD interval width, 95% HPD interval coverage rate and  $\ell_1$  error evaluated via 10,000 bootstrap samples. Overall, GB-NPMLE Algorithm 3 produces NPMLE bootstrap samples that are nearly indistinguishable from standard NPMLE bootstrap. Also in table 3, the required computational time to achieve 10,000 bootstrap samples is reported where sample size  $n \in \{100, 1000, 10000\}$ . Standard NPMLE bootstrapping becomes very challenging

when dealing with a large-size dataset, such as  $n \geq 10,000$  (nearly 12 hours above). GB-NPMLE Algorithm 3, on the other hand, excels at computing NPMLE bootstrap samples at least ten times quicker i.e  $\leq 10$  minutes even when  $n = 10,000$ . Although NPMLE inference in context of Binomial mixture model is quite efficient (even when the number of trials  $n \geq 1,000$ ), GB-NPMLE (Algorithm 3) shows a promising overall computational efficiency and generates well-approximated bootstrap samples for statistical inference.